Draft version October 6, 2020
Typeset using LaTeX **twocolumn** style in AASTeX63

Classifying Be star variability with TESS I: the southern ecliptic

Jonathan Labadie-Bartz,[1] Alex C. Carciofi,[1] Tajan Henrique de Amorim,[1] Amanda Rubio,[1] André Luiz,[1] Pedro Ticiani dos Santos,[1] and Thomson-Paressant Keegan[2]

[1]*Instituto de Astronomia, Geofísica e Ciências Atmosféricas, Universidade de São Paulo, Rua do Matão 1226, Cidade Universitária, 05508-900 São Paulo, SP, Brazil*

[2]*LESIA, Paris Observatory, PSL University, CNRS, Sorbonne University, Université de Paris, 5 place Jules Janssen, 92195 Meudon, France*

Submitted to AAS Journals

ABSTRACT

High-quality TESS photometry is analyzed for a sample of 443 classical Be stars observed in the first year of the mission. The often complex and diverse variability of each object in this sample is classified to obtain an understanding of the behavior of this class as a population. 98% of the systems are variable above the noise level, with timescales spanning nearly the entire range of what is accessible with TESS, from tens of minutes to tens of days. Although Be star behavior is diverse, the picture painted by TESS of their variability as a population is summarized as follows. Nearly every system contains periodic signals in the frequency regime between about 0.5 – 4 d^{-1}, and in most cases there is clear evidence for multi-periodicity, suggestive of non-radial pulsation. One or more groups of closely-spaced frequencies is the most commonly observed feature, present in 81% of the sample. Among the Be stars with brightening events that are characteristic of mass ejection episodes (17% of the full sample, or in 29% of early-type stars), the majority of these (78%) show temporarily enhanced amplitude in one or more frequency groups coinciding with the secular brightening. About one third of the sample is dominated by low frequency ($f < 0.5$ d^{-1}, and often much lower) variability. Stochastic signals are prominent in about 30% of the sample, with varying degree of intensity. Higher frequency signals ($6 < f < 15$ d^{-1}), usually in addition to the aforementioned groups of relatively lower frequencies, are sometimes seen (in 15% of the sample) and in most cases likely reflect p mode pulsation. In rare cases (∼5%), even higher frequencies beyond the traditional p mode regime ($f > 15$ d^{-1}) are observed. The main goal of this work is to quantify this behavior for the Be star population at large and provide the appropriate context for the interpretation of the observed signals and their incidence rates according to coarse spectral types provided by the literature.

1. INTRODUCTION

Classical Be stars have been studied for over 150 years, yet key aspects of their nature remain veiled. Since their discovery in 1866 (Secchi 1866), it has been established that classical Be stars (here after simply Be stars) are non-supergiant B-type stars with rapid, near-critical rotation, and are in general non-radial pulsators, which non-radiatively eject mass to form a viscous, near-Keplerian circumstellar "decretion" disk from which characteristic spectral emission features arise (Rivinius et al. 2013, and references therein). While significant progress has been made in the past many decades, the following questions regarding remain outstanding in general: How do they acquire such fast rotation? Why do they pulsate the way the do? How does rapid rotation influence internal processes such as angular momentum transport and chemical mixing? How are matter and angular momentum ejected at sufficiently high amounts? How does this ejected matter organize itself around the star on a geometrically thin and mostly Keplerian disk?

To understand the physical processes of Be stars is to better understand stellar evolution, structure, and behavior as a whole. Mass, rotation, binarity, metallicity, and magnetic fields are the primary factors that dictate the life of a star. Be stars span the entire spectral type range from late O to early A, do not host large-scale magnetic fields down to a detection limit of about 50 – 100 Gauss (Wade et al. 2016, in a sample of 85 Be stars), are more common in lower metallicity environments (Maeder et al. 1999; Wisniewski & Bjorkman 2006; Peters et al. 2020), and are the most rapidly rotating non-degenerate class of objects known, on average rotating at or above 80% of their critical rotation rate (Frémat et al. 2005; Rivinius et al. 2013). The binary fraction and binary parameters of Be stars as a population are somewhat uncer-

Corresponding author: Jonathan Labadie-Bartz
jbartz@usp.br

tain, but there is evidence that the binary parameters are similar to that of B type stars in general (Oudmaijer & Parr 2010), as well as suggestions that a very high fraction of Be stars exist in binaries (Klement et al. 2019). Be stars then represent critical test beds, especially for theories that explain the role of rotation in stars, which to date remain insufficiently developed for rapid rotators.

In general, there are two plausible channels that lead to the rapid rotation of Be stars. One of these is via binary interaction, where material and angular momentum is transferred to the present-day Be star by an initially more massive companion. The result of this evolutionary stage is a rapidly rotating Be star and either a hot subdwarf (an sdOB star), such as Phi Per (Thaller et al. 1995), HD 55606 (Chojnowski et al. 2018), and FY CMa (Peters et al. 2008), or a stellar remnant – a black hole (Casares et al. 2014), neutron star (Rappaport & van den Heuvel 1982), or a white dwarf (although no Be + white dwarf binaries are known). Alternatively, a single star evolutionary channel remains viable for Be stars, where their angular momentum content is inherent in their formation and subsequent evolution (Zorec & Briot 1997). Which of these two channels dominates remains unknown.

Space photometry has led to significant advances in the field of Be stars in recent years. Analysis of space-based photometry has revealed that pulsation is ubiquitous among classical Be stars, and that they pulsate primarily in low order g modes where gravity is the restoring force (Rivinius et al. 2003), similar to the class of Slowly Pulsating B (SPB) stars. Higher frequency p modes (pressure being the restoring force) are are also observed in some Be stars, but are less common than g modes. Rossby waves (r modes, where centrifugal forces dominate) may also be present in Be stars (Saio 2013; Saio et al. 2018b). Analysis of photometry from the MOST (Walker et al. 2003), BRITE (Weiss et al. 2014), Kepler (Koch et al. 2010), and CoRoT (Baglin et al. 2006) satellites has shown that the frequency spectra of Be stars are often complex relative to other B-type main sequence pulsators (the β Cephei and SPB stars), typically exhibiting multiperiodicity, groups of closely-spaced frequencies (as well as isolated frequencies), signatures of stochastic variability, and long-term (usually aperiodic) trends (Baade et al. 2017, 2018; Rivinius et al. 2016; Semaan et al. 2018; Walker et al. 2005a). The fact that virtually all Be stars pulsate suggests that pulsation is an important aspect of these systems, and is also a potentially useful probe of their interiors via asteroseismology. High precision space photometry therefore represents a valuable tool to study the physics of Be stars and to learn about the role of rapid rotation in stellar structure and evolution.

Both the central star and the disk are interesting astrophysical systems. While the star forms the disk, the evolution of the disk is largely independent of the star itself, being primarily influenced by the gravitational and radiation fields of the star. Once a disk is formed, the material forgets its history and evolves mainly through viscous forces (Lee et al. 1991; Carciofi 2011; Rímulo et al. 2018), and disk observables can be used to estimate the viscosity parameter (α) and the flow of mass and angular momentum out of the system. Radiative ablation will also contribute to the evolution (more specifically the destruction) of the (inner) disk (Kee et al. 2016), especially in the hottest OBe stars, but the degree to which this contributes to disk evolution is poorly constrained at present. Meanwhile, the central star represents the best opportunity to study the physics of rapidly rotating main sequence pulsating stars. In order to learn from the star, the disk, and the star-disk interface, it is necessary to disentangle their relative contributions to a given observable.

The Transiting Exoplanet Survey Satellite (TESS; Ricker et al. 2015) mission, launched in 2018, has opened a new window into massive star variability. The Kepler spacecraft dramatically advanced the state of the art of stellar variability with its unprecedented photometric precision and long (4 years) observational baseline of a single field (Borucki et al. 2010). However, due to its observing strategy, only a small number of relatively faint OB stars were observed. While TESS has the same general goal as Kepler, the discovery of transiting exoplanets, its observing strategy is markedly different, at great benefit to the study of massive stars. In its prime mission, TESS covers ~74% of the sky in two years, with a large field of view that shifts approximately every 27 days. Unlike Kepler, the TESS sectors have significant overlap with the galactic plane, where the vast majority of OB stars are found. Whereas Kepler observed only 3 known Be stars (Rivinius et al. 2016), TESS is observing over 1000. Another benefit is that the TESS mission was designed for brighter stars ($V \lesssim 12$), which means that the systems viewed by TESS have more comprehensive historical datasets and are more practical to observe from the ground.

Capitalizing on the strengths of TESS, the main goal of this work is to provide an overview of the variability seen in the population of ~500 Be stars observed in the first year of the TESS mission at a high precision and at short timescales (tens of minutes to weeks). Variability characteristics are ascribed to every star in the sample, providing insight to the behavior of the population as a whole and bringing to light patterns that exist according to spectral type and correlations between the different variability characteristics. In this context, the most typical signals are those of stellar pulsation which manifest as periodic signals in the flux of a given system. As has been reported in many studies, such periodic signals often form "frequency groups" in the observed power spectra (*e.g.* Baade et al. 2018; Rivinius et al. 2016; Semaan et al. 2018; Walker et al. 2005a). These frequency groups are in general the most characteristic signature of Be stars

observed with space photometry. In addition to photospheric signals, TESS is also sensitive to changes in the circumstellar environment close to the star, which can be associated with episodes of mass ejection (with the matter perhaps being inhomogeneously distributed in azimuth).

In section 2, the TESS satellite and its data products are introduced, and methods for data extraction are described. Section 3 describes the analysis methods and shows example results of these methods for artificial light curves. Section 4 introduces the characteristic features seen in the TESS data of Be stars, which are then used to describe each star in the sample. The results of the analysis of these signals are presented in Section 5, including discussion of each characteristic and the relevant astrophysical context. In Section 6 a broad overview is given with an emphasis on correlations between the different variability classifications presented in Section 5, followed by concluding remarks in Section 7.

2. DATA

The NASA Transiting Exoplanet Survey Satellite (TESS; Ricker et al. 2015) is a photometric mission performing wide-field photometry over nearly the entire sky. The 4 identical cameras of TESS cover a combined field of view of 24° × 96°. During the first year of TESS operations, nearly the entire southern ecliptic sky was observed in 13 sectors, with each sector being observed for 27.4 days. Some regions of the sky are observed in multiple sectors. TESS records red optical light with a wide bandpass spanning roughly 600 – 1000 nm, centered on the traditional Cousins I-band. For optimal targets, the noise floor is approximately 60 ppm hr^{-1}.

Full Frame Images (FFIs) from TESS are available at a 30-minute cadence for the entire field of view, allowing light curves to be extracted for all objects that fall on the detector. Certain high priority targets were pre-selected by the TESS mission to be observed with 2-minute cadence, some of which were chosen from guest investigator programs. For the sample studied in this work, light curves were extracted from the FFIs for all systems, and 2-minute cadence light curves were also used whenever available. Generally the 30-minute and 2-minute light curves contain the same signals, which bolsters our confidence in the methods used for the FFI light curve extraction. However, there are some subtle differences which are further explained in the following subsections.

2.1. *Extracting light curves from TESS FFIs*

Light curves are extracted from the TESS FFIs using three different methods. This is done to increase our confidence in results when these methods produce LCs that agree, and also decreases the incidence of false-positive detections of signals if they exist in only one version of the extracted LC, being perhaps caused by imperfect removal of systematic trends or blending from neighboring objects.

The first method used to extract LCs begins by using the lightkurve package (Lightkurve Collaboration et al. 2018) and TESScut (Brasseur et al. 2019) to download a target pixel file (TPF) with a 50 × 50 pixel grid centered on the target star's coordinates for every available TESS sector. An aperture threshold of 10 sigma relative to the median flux level is used as a first step to automatically determine the aperture mask for the target star. The size of the target pixel mask is allowed to scale with stellar brightness. All pixels outside of a 15 × 15 pixel exclusion zone (centered on the target star) are then used as regressors in a PCA analysis to remove common trends across this region of the CCD. The result is a PCA detrended light curve that is largely free from systematic trends. At the same time, an alternate version of the light curve is produced, using only background removal, since in some instances a PCA detrending method will remove astrophysical variations in the target star with timescales of days or longer.

The third method uses the Astroquery (Ginsburg et al. 2019) routine Catalogs to identify five stars of similar brightness on the same CCD as the target star within an annulus of an inner radius of 0.1 degree and an outer radius of 0.35 degrees (although this is allowed to vary if there are two few stars of sufficient brightness within the original annulus). TESScut is then used to extract a light curve for the target star and all of the identified neighboring stars using a 3 × 3 grid of pixels. The trend filtering algorithm (TFA) in the VARTOOLS light curve analysis package (Hartman 2012) is then used to identify and remove trends that are common to the set of the target star and its neighbors. This aperture is almost always smaller than that used in the PCA method, and is therefore less susceptible to blending (at the cost of achieving a lower SNR due to excluding some flux-containing pixels).

In some cases one of the above methods will fail partially or completely (most often when a target is close to the edge of a detector, or in the most crowded fields). Using different extraction methods allows us to determine when this is the case so that improperly reduced data is flagged as such. The first method using lightkurve tends to be more reliable and produces a light curve with higher signal-to-noise ratio (SNR), and all plots of 30-min cadence data shown in this work use this version of the light curve. The sampling rate of 30 minutes allows for the detection of frequencies up to 24 d^{-1}.

2.2. *2-minute cadence light curves*

About 65% of our sample has 2-minute cadence light curves (LCs) available from the TESS office. When these LCs exist, we performed the same analysis as was done for the LCs extracted from the FFIs. In nearly all cases, the results are virtually identical between different versions of the LC. We use the Pre-search Data Conditioning Simple Aper-

ture Photometry (PDCSAP) flux from the TESS LCs, which is calibrated in a way that removes long term trends. This generally yields a cleaner version of the LC (compared to the Simple Aperture Photometry (SAP) flux) that is well suited for frequency analysis. The disadvantage is that the detrending process may remove astrophysical variability on relatively long timescales. These, however, can easily be identified in the 30-minute data. For that reason both sets of data were always analysed for all stars for which they are available. The higher cadence 2-minute LCs allow for the detection of much higher frequencies relative to the data extracted from the FFIs, up to the Nyquist limit of 360 d^{-1}.

2.3. *Sample selection*

The Be Star Spectra (BeSS) database[1] (Neiner et al. 2011) was used to create a list of Be stars between V-mag of 4 – 12. The sample of Be stars from Chojnowski et al. (2015) was also included. Only targets in the southern ecliptic hemisphere were chosen, in order to match the fields observed by TESS in its first year of operations. This initial list of 548 stars was reduced to 443 by rejecting systems known or strongly suspected to be something other than a classical Be star (*e.g.* interacting binaries or B[e] stars), and stars for which there are no TESS data or the data is of insufficient quality (*i.e.* when a star falls into a gap between sectors, or systematic effects or unusually high noise levels severely hamper our ability to analyze a given LC). Of these 443 classical Be stars, 223 (50%) are of early type (B3 and earlier), 80 (18%) are mid type (B4, B5, and B6), 120 (27%) are late type (B7 and later), and 25 (6%) are of unknown spectral type.

The vast majority of these targets also have years-long light curves from the ground-based Kilodegree Extremely Little Telescope (KELT, Pepper et al. 2007, 2012), where the data for some of the TESS sample are published and available in Labadie-Bartz et al. (2017, 2018). While the KELT data was not directly used in the analysis of these systems in this work, in some instances it was used to corroborate long term trends or periodic signals seen in TESS, or to confirm systems that are not Be stars (*e.g.* binaries with ellipsoidal variation). Further works studying these systems should take advantage of the more comprehensive suite of time-series data provided by TESS, KELT, BeSS, APOGEE, and perhaps other sources.

3. ANALYSIS

A variety of methods were used to analyze the sample. Standard Fourier methods lie at the core of the analysis, but the diversity of signals expressed by Be stars demands a careful analysis, including visual inspection of the light curves, separately considering different frequency regimes, measuring aperiodic variability, tracing variable amplitudes of periodic signals, and documenting correlations in time between different signals. Consideration is also given to the degree of blending, and potential issues from saturation, systematic effects, and noise. Details about the data analysis are described in the following subsections.

3.1. *Removing outliers and bad data*

Because of the variety of signals in the data, especially in systems exhibiting longer term trends of relatively high amplitude, outliers cannot be removed through standard methods such as sigma clipping. Instead, outliers and sections of poor quality data were removed in the following way. After reconstructing the light curve with a sum of Fourier terms, the calculated fit was subtracted from the observed data, and points greater than five times the median absolute deviation from the median of the residuals were automatically identified as outliers. At this stage, the observed and calculated data and the residuals were manually examined, allowing for the possibility of removing additional sections of poor-quality data. These cleaned light curves, with outliers and sections of poor quality data removed, are used in all following analysis steps.

3.2. *Lomb-Scargle periodograms and pre-whitening*

Because of the generally complex nature of photometric variability of Be stars, there are signals with a wide range of timescales and behavior that we are interested in measuring which requires extra analysis steps. For example, in a system with significant aperiodic low-frequency variability, it is prudent to detrend against these signals when analyzing the data for higher frequency signals. Through iterative pre-whitening, each sector of data for each object was detrended against all signals lower than 0.5 d^{-1} up to a false alarm probability of 10^{-2} (in a similar fashion as Rivinius et al. 2016). A frequency analysis was then performed for the entire set of TESS observations for each star, separately for the original and detrended versions of the light curves. The TIMESERIES.LOMBSCARGLE package (VanderPlas et al. 2012; VanderPlas & Ivezić 2015) of ASTROPY (Astropy Collaboration et al. 2013, 2018) was used to compute these Lomb-Scargle Periodograms (LSPs). The above procedure was applied to both the 2- and 30-minute cadence data, when available.

To determine the individual frequencies present in the data, the VARTOOLS light curve analysis software with the LOMB-SCARGLE routine (Zechmeister & Kürster 2009; Press et al. 1992) was used to detect and iteratively pre-whiten the data against each recovered signal (up to a false alarm probability of 10^{-2}), recording the frequency, phase, amplitude, SNR, and false alarm probability. The frequency and amplitude of these signals are used to plot the pre-whitened periodograms,

[1] http://basebe.obspm.fr

and are also used to re-construct each light curve based on the recovered signals, which are visually compared to the original photometric data to ensure a good fit from the Fourier analysis. These methods are similar to what is typically done for space photometry of Be stars, *e.g.* with MOST (Walker et al. 2005a), Kepler (Rivinius et al. 2016), and CoRoT (Semaan et al. 2018).

3.3. *Wavelet plots*

It is common for Be stars to show photometric signals that vary in amplitude over time. Wavelet plots are a convenient way to visualize this, as they depict the frequency spectrum as a function of time (at the cost of a degraded frequency resolution). The Python package SCALEOGRAM[2] was used to perform a wavelet analysis for each star, considering the original and low-frequency detrended (signals with frequencies < 0.5 d^{-1} removed) versions of the data separately.

3.4. *Testing Artificial Light Curves*

In order to better understand the signals that are recovered from TESS light curves of Be stars, tests were performed where artificial signals are injected into the data and then recovered. This process begins by taking a TESS light curve of a typical Be star from a single sector, and removing all signals through iterative pre-whitening, leaving a light curve that contains only noise. Signals are then injected, and the light curve is analyzed using the same methods that are applied to the real data. The injected signals were motivated by common features seen in the data for Be stars.

In the first trial, nine sinusoidal signals with different but constant amplitudes are injected into the pre-whitened light curve in two groups, with four signals centered around 2 d^{-1}, and five signals centered around 3.3 d^{-1} to imitate the frequency groups that are commonly seen in Be stars (the amplitudes of these signals are between 0.2 – 1 ppt).

The artificial light curve is then analyzed through iterative pre-whitening. All of the injected signals are recovered, with the mean difference between the injected and recovered frequencies being 0.06%, and the recovered amplitudes are precise to within 10%. However, other signals are also found in the analysis. These spurious signals are all close to the injected frequencies and lie within their respective groups. Panel 'A' of Figure 1 shows the Lomb-Scargle periodogram and the signals recovered through iterative pre-whitening of this first artificial light curve, with the location of the injected signals also marked. Only one frequency group is shown for clarity, as the behavior of the other group is qualitatively the same. In the following trials, only this group near 3.3 d^{-1} is modified, and there is no discernible influence on regions of the frequency spectrum that are not shown in Figure 1.

[2] https://github.com/alsauve/scaleogram

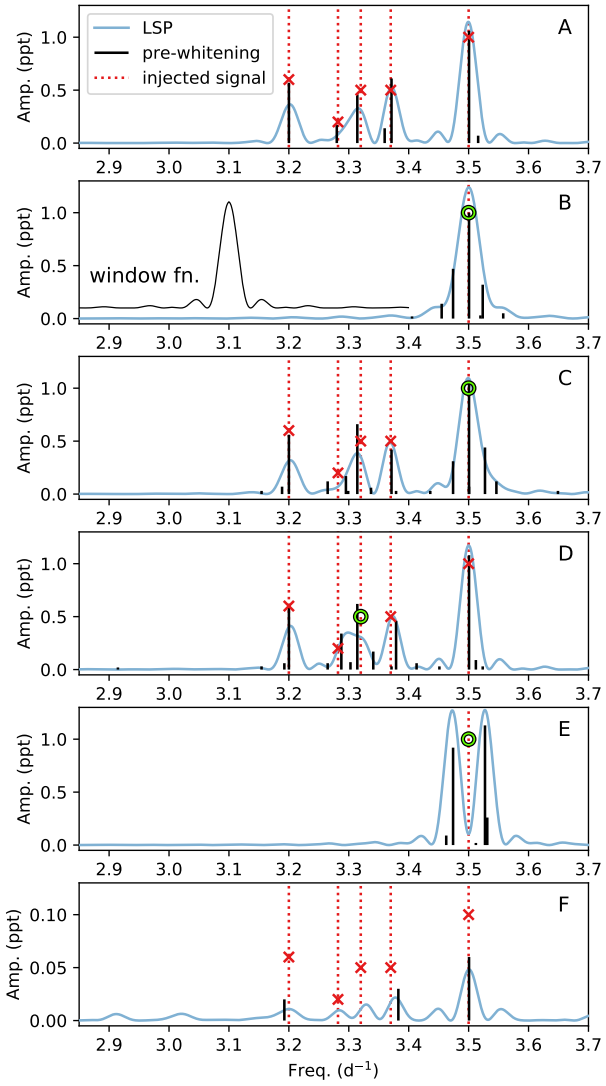

Figure 1. Analysis of an artificial light curve with known signals injected. The location of injected signals are shown with red dotted vertical lines, with amplitudes of constant signals marked by a red x, and the maximum amplitude of signals that vary in strength with time is marked by a green circle. The Lomb-Scargle periodogram of the artificial light curve is shown in light blue, and the signals found through iterative pre-whitening of the artificial light curve are vertical black lines, where their height reflects the amplitude of the recovered signal. The window function (with arbitrary vertical scale), centered at 3.3 d^{-1}, is shown in panel B. Note that each sector will have a slightly different window function, and for systems viewed in multiple sectors the window function becomes more narrow. *A:* A frequency group where all injected signals have a constant amplitude. *B:* A single frequency with a linearly decreasing amplitude is injected. *C:* The same as panel A, but the strongest signal at 3.5 d^{-1} has a linearly decreasing amplitude. *D:* The same as the panel A, but the middle signal at 3.32 d^{-1} has a linearly decreasing amplitude. *E:* The same as the panel B, but the amplitude is modulated by a sinusoid. *F:* The same as panel A, but all amplitudes are smaller by a factor of ten.

Next, a single frequency at 3.5 d^{-1} is injected into the light curve with an amplitude that decreases linearly from 1 ppt to reach an amplitude of 0 at the end of the light curve. Panel 'B' of Figure 1 shows this trial. The injected frequency is recovered to within 0.02% with an amplitude indistinguishable from that of the injected signal at its strongest. Other signals are also found close to the injected frequency and with amplitudes decreasing with distance from this frequency. These signals are weaker than the injected single frequency, but are still significant relative to the noise level. The periodogram peak is also wider than it would be if the amplitude were not modulated.

The original nine signals are again injected, with the strongest (at 3.5 d^{-1}) being modulated in amplitude in the same way as the second trial. Again, there are spurious peaks near 3.5 d^{-1} caused by the amplitude modulation, but now there are additional peaks in the group that did not exist in the first trial, and one of the injected signals (the second in the group, at 3.282 d^{-1}) is not properly recovered. Panel 'C' of Figure 1 shows this.

This test is repeated, but with the amplitude of the 3.5 d^{-1} signal being constant and the amplitude of the middle frequency of the group, at 3.32 d^{-1}, linearly decreasing at the same rate as the second and third trials. Spurious peaks appear, and the precision with which the five injected signals of the group are recovered is degraded, as shown in panel 'D' of Figure 1.

A trial similar to the second one is done, but instead of a single frequency with a linearly decreasing amplitude, the amplitude is modulated by a sinusoid with a frequency of 0.0275 d^{-1}. In this case, the original injected frequency at 3.5 d^{-1} is not recovered, but rather two strong peaks appear in the periodogram (panel 'E' of Figure 1). This is explained by the trigonometric identity $\sin(\alpha) * \sin(\beta) = [\sin(\alpha - \beta) - \cos(\alpha + \beta)]/2$. In other words, with a standard Lomb-Scargle analysis alone it is impossible to distinguish between a single frequency, β, whose amplitude is modulated by some lower frequency, α, and two signals of constant amplitude located at $\beta - \alpha$ and $\beta + \alpha$. In principle this can be remedied by also considering phase information. However, we do not perform such an analysis in this work.

Finally, the first trial was repeated but with all amplitudes being smaller by a factor of 10 (panel 'F' of Figure 1). With these amplitudes approaching the noise floor of the data, the injected signals are poorly recovered. This demonstrates a practical, but approximate, lower limit on the amplitude of signals that can be reliably recovered in a typical TESS light curve is ~0.05 ppt[3].

The first trial, where the injected signals that make up two groups all have a constant amplitude, is shown in more detail in Figure 2. The wavelet analysis of this artificial light curve shows that the two groups are variable in power over time. However, this is solely a consequence of the beating phenomenon between signals in a given group, since each injected signal is known to be constant in amplitude. The beating can also be seen as a corresponding change of the overall amplitude in the light curve itself.

Numerous other similar tests were performed, but the above examples serve to demonstrate the overall results of attempting to recover signals in groups of closely spaced frequencies when amplitudes are allowed to vary (as is often the case with Be stars). The main conclusions of these tests are that the methods used to detect signals in the TESS data will almost always result in some spurious signals whenever there are groups of frequencies and signals with varying amplitudes can, sometimes dramatically, compound this effect. While the frequency groups themselves, and usually the strongest frequencies comprising them, are reliably recovered, some degree of spurious detections is inevitable. Complex beating patterns can exist within a frequency group, causing apparent modulation of the strength of the group over time despite all individual signals having a constant amplitude. Therefore, caution must be exercised when analyzing TESS data for Be stars, and these limitations must be kept in mind when considering the often complex light variability seen in this sample. While these limitations are well known in general, the complex nature of Be star variability and the low frequency resolution of most TESS light curves exacerbates such issues.

3.5. *Interpreting observations of Be star systems*

Certain observed variations can be confidently attributed to either the star or the disk. In terms of photometry, brightening or fading events that occur on timescales of months or years are understood to be due to disk growth or dissipation, while coherent, stable periodic signals on timescales of around one day and less are best attributed to stellar pulsation. There are, however, many cases where photometric signals are ambiguous in origin. The stellar rotation period, orbital period in the close circumstellar environment, and possible pulsational periods are all very similar. Since many factors can influence the total brightness of the system (and other observables) in often complex and time-variable ways, care must be taken

[3] A true lower limit depends on the brightness of the target, how successfully systematic trends are removed, the details of the frequency spectrum in the vicinity of a given signal, the number of sectors in which the target was observed, the choice of aperture used to extract the light curve, and perhaps other factors.

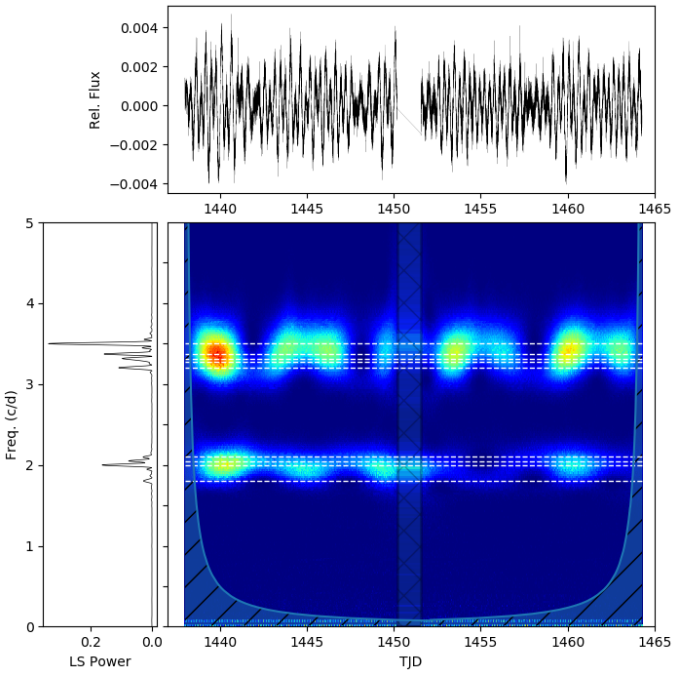

Figure 2. Artificial light curve (top), LSP (left), and wavelet plot (middle) for the first trial discussed in Section 3.4 with two frequency groups, with each signal having a constant amplitude. The wavelet plot shows both groups having apparently variable power, which is solely a consequence of the beating phenomenon. In the wavelet plot, horizontal dashed lines mark the injected frequencies, and regions occupied by hash marks denote gaps in data and regions where wavelet signals are otherwise unreliable due to edge effects.

in interpreting photometric data. In the following, examples are provided of variability that can be firmly connected to either the disk or star, but debatable cases are also discussed, in order to highlight both the great potential, as well as the complications ensuing from interpreting space photometry alone.

4. CHARACTERISTIC FEATURES OF BE STARS IN TESS

The main goal of this work is to assign characteristic variability features to each star in the sample, and to then use these characteristics to describe the sample as a population. This section introduces these features and shows examples.

4.1. *Light curves and their frequency spectra*

Most of the characteristic features in the TESS data of Be stars can be inferred by inspecting the light curve and the Lomb-Scargle periodogram as a measure of the frequency spectrum. While each light curve and frequency spectrum is unique, there are certain features that are common among many members of the sample. Fig. 3 shows examples of Be stars that show these characteristic features, which we introduce and describe here.

In what follows, we adopt a convention where low frequencies are those less than 0.5 d^{-1}, mid frequencies are between 0.5 – 6 d^{-1}, high frequencies are between 6 – 15 d^{-1}, and very high frequencies are greater than 15 d^{-1}. While these distinctions are somewhat arbitrary, they are physically motivated. Low frequency signals are generally below those of typical g mode pulsation in Be stars, mid (high) frequencies span the typical range of g mode (p mode) pulsation in Be stars, and very high frequencies are above the typical p mode regime in Be stars (*e.g.* Handler 2013; Bowman 2020, and references therein). While the rapid rotation (and evolutionary stage) of Be stars can complicate this simplified scheme, it is useful to choose cutoffs to delineate these categories in order to classify the observed variability.

- Flickers: We loosely define "flickers" as features in the light curve whereby the brightness increases or decreases by a few percent over a few days, followed by a return towards baseline. Some flickers show a precursor phase, i.e., a dimming before the rising in brightness, and some flickers are accompanied by a temporary increase of the amplitude of higher frequency signals (or their emergence if not already present). The largest amplitude features in panel B of Fig. 3 are examples of this. Flickers are not an oscillation around the mean brightness (like in panel C), but are rather a marked departure from the baseline brightness.

- Low-frequency signals dominate: Features with frequencies lower than 0.5 d^{-1} are the most prominent type of variation in the data. Panel B in Fig. 3 is an example of this characteristic. This is usually apparent from the light curve, but can be more quantitatively determined if the strongest periodogram signals are in the low frequency regime.

- Frequency groups: Many closely-spaced frequencies often form groups in the frequency spectra of Be stars. The system in panel D shows three well defined groups near 0.05, 1.2, and 2.4 d^{-1}, and panel E shows two groups near 3 and 6 d^{-1}. Panel B and F also show two frequency groups each. There is one group in panel A (near 2 d^{-1}) plus stochastic variation at lower frequencies. Panel C is more ambiguous as plotted, but shows two prominent groups near 0.6 and 1.4 d^{-1} which are more easily identified through iterative pre-whitening and acknowledging that the periodogram peaks are wider than the window function, suggesting they contain multiple un-resolved signals. For each star with groups, the position and relative strength of the groups are recorded, as is the approximate "center of mass" and "mass" of the group (defined in Section 4.4). The typical configuration of frequency groups consists of

two groups, $g1$ and $g2$, where $g1$ usually is found between 0.5 – 3.0 d^{-1}, and $g2$ is located at approximately twice the central frequency of $g1$. There is often, but not always, a low frequency group, $g0$, centered at < 0.5 d^{-1}. When groups exist for some object, we record the total number of groups and whether or not they are in this typical configuration. It is common for a harmonic series of groups to extend from the typical $g1$ and $g2$, usually with decreasing amplitude.

- Stochastic variation: Non-periodic variability is a significant feature of the data. Stochastic signals can appear as extra "noise" in the frequency spectrum (as opposed to coherent periodic signals, which exist at a single frequency) that is strongest at the lowest frequencies, and decreases towards higher frequencies. However, this "red noise" is astrophysical, and arises from genuine variability which is not periodic. Panel A shows an example that includes stochastic variability. The forest of signals between 0 – 2 d^{-1} in the periodogram is stochastic in nature, while the frequency group just above 2 d^{-1} is a separate (periodic) feature. Panel B likewise includes stochastic variability (manifesting as an underlying "continuum" of signals at low frequencies in the periodogram) in addition to frequency groups composed of periodic signals that clearly stand above the local noise.

- Single, isolated frequencies: In contrast to groups, some frequencies are singular and well-defined. There are many isolated frequencies in the periodogram of panel F, and also some in panel A (with low amplitudes).

- High and very high frequency signals: Systems that exhibit periodic signals in the high ($6 < f < 15$ d^{-1}) and very high ($f > 15$ d^{-1}) frequency regime are recorded. Panel F shows a star with many of these high and very high frequency signals, while panel A also meets the criteria of having high frequency signals. Harmonics alone are not considered here, nor are near-harmonic sequences of groups that begin at mid frequencies. For example, if there is a signal at 4.0 d^{-1} with an exact harmonic at 8.0 d^{-1}, we do not classify this as a high frequency signal since the presence of this harmonic may simply indicate that the fundamental signal is not perfectly sinusoidal. In panel E, the groups near 6 d^{-1} and 9.5 d^{-1} are the second and third groups in a series that begins with $g1$ near 3 d^{-1}, and thus this star does not meet the criteria for having high frequency signals.

- Harmonics of isolated signals: Some frequency spectra show clear harmonics, where a signal is found at an integer number times the frequency of another signal. In some cases these harmonics are exact, while in others they are approximate. An exact harmonic is seen in panel F, where the lowest frequency, $f_0 = 1.684$ d^{-1} has a first harmonic at $2\times f_0 = 3.368$ d^{-1} (and increasingly smaller amplitude second, third, and fourth harmonics). Frequency groups often have (multiple) harmonics, but those are considered separately.

- No detected signals: A small fraction of the stars in the sample show no variability above the TESS noise level. This is generally restricted to later spectral types, where it is well known that amplitudes are relatively low.

4.2. *Time variable signals*

While traditional light curve and Lomb-Scargle analysis provide valuable information about the signals present in the data, it is clear from Fig. 3 that some signals are variable in time. For example, in panels B, C, and D, the amplitude of the strongest modes are clearly variable. In a given light curve, some signals can be constant, variable and (anti-) correlated, or variable and apparently uncorrelated. Sometimes transient periodic signals appear and disappear, which can be correlated with other signals in the light curve (*e.g.* frequency groups corresponding to the appearance of flickers). For these reasons, it is necessary to analyze the behavior of signals over time to get a more complete picture of the variability seen in a given system.

Figure 4 shows an example with time variable signals. The frequency groups near 2 d^{-1} and 4 d^{-1} increase in amplitude at around the same times the system undergoes secular brightening events (*i.e.* the amplitude of these groups are positively correlated with flicker events, and with each other). The time variable signals we consider are described here.

- Frequency group variability : When frequency groups exist, their strength is examined as a function of time and we classify the behavior of the two main groups as being either
  - stable (having a constant amplitude)
  - variable due to beating
  - variable in an unclear pattern
  - present for only some portions of the light curve, and absent for others (or at a significantly lower level for lengths of time inconsistent with beating). These may, for example, be associated with flickers.

- Flickers + enhanced amplitudes: Some systems see an enhancement in amplitudes of frequencies or groups

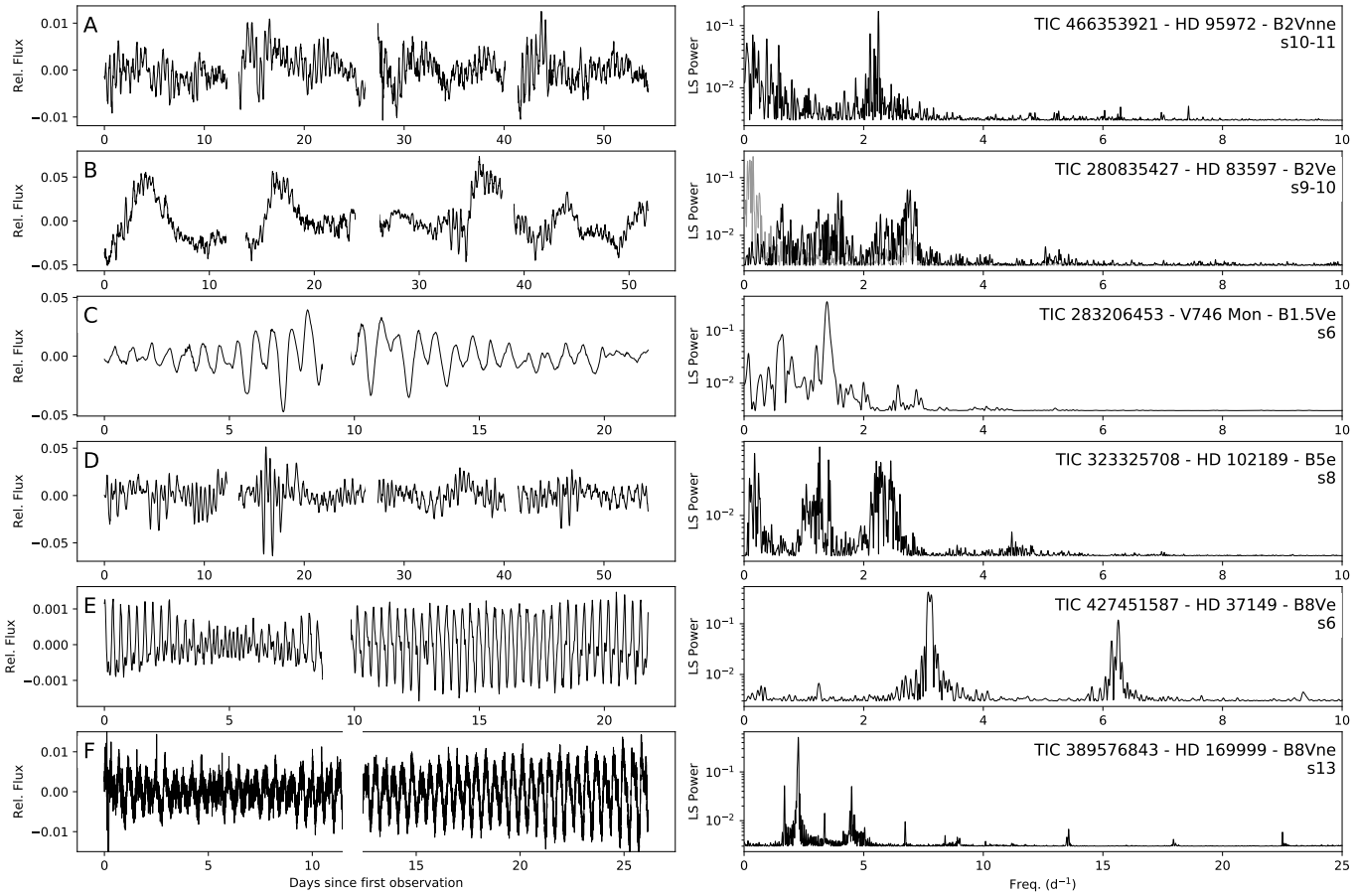

Figure 3. TESS light curves (left) and Lomb-Scargle periodograms (right) for a representative selection of Be stars that show certain characteristic features, as described in Sec. 4. For panel B, the periodogram is re-calculated after removing the low frequency (< 0.5 d^{-1}) signals (which are shown in a lighter grey color). Panel F uses 2-minute cadence data, which better emphasizes the highest frequency signals. All other panels use 30-minute cadence data. The frequency axis of the periodogram in panel F is extended to include the high frequencies. Signals at frequencies higher than 10 d^{-1} are absent in all other stars shown here. The TIC ID, common ID, spectral type, and TESS sectors are printed in the periodogram plots.

correlated to secular increases in brightness (*e.g.* in Figure 4). For all systems that show flickers, we record whether or not there is an associated enhancement in group amplitude(s). This is a specific case of the above category, where a group may be present for only some portion of the observations.

- Correlations between groups: The strength of the two main groups ($g1$ and $g2$, if they exist) are examined over the duration of the light curve and compared. We determine if the groups
  - are positively correlated (*e.g.* Figure 4)
  - are negatively correlated
  - are not apparently correlated (*e.g.* Figure 5).
  - may or may not be correlated, but their relationship is unclear (*e.g.* Figure 2).

4.3. *Interpreting results of our analysis*

After identifying the characteristic features of interest, plots for the sample were visually inspected in order to determine which of the above characteristics can be attributed to each star and other information about the signals that are present (*e.g.* the location and relative strength of frequency groups).

There is some degree of subjectivity in assigning variability classifications. Each object was analyzed in detail independently by three authors of this work. If a consensus was reached regarding a given classification, then that classification was assigned to the system. If there was disagreement or uncertainty, then the object was inspected in more detail and a final decision was made regarding the classification in question. In some cases, it remained not possible to confirm or reject a given classification.

An important aspect of this manual analysis was determining if a given object is not a classical Be star. To this end,

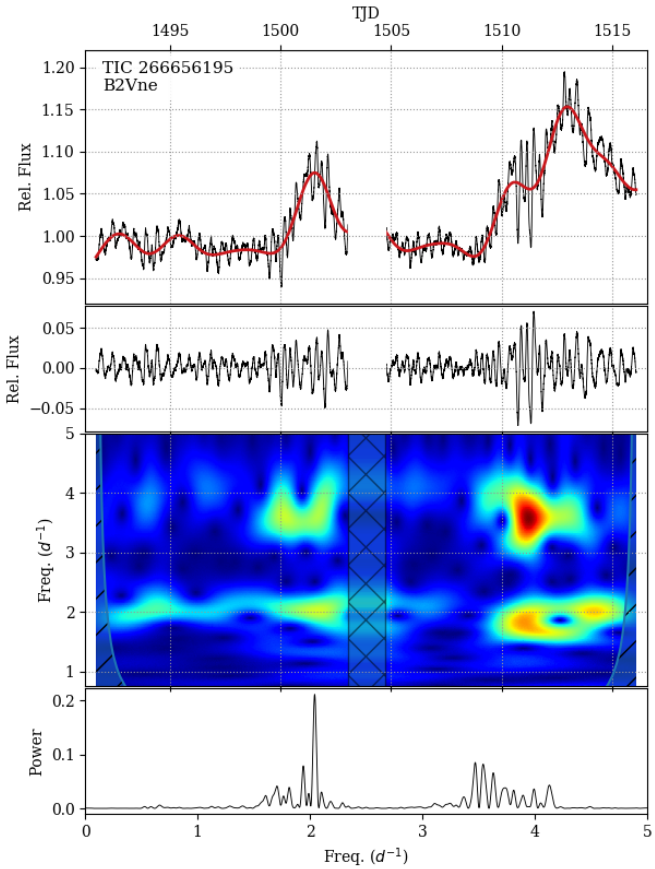

Figure 4. A system where flickers correspond to the enhancement of the two main frequency groups. *First:* 2-minute cadence LC (black), with the low frequency signals in red. *Second:* The LC after removing low frequency signals. *Third:* Wavelet analysis. *Fourth:* Lomb-Scargle periodogram. The top three panels share the same x-axis (TJD).

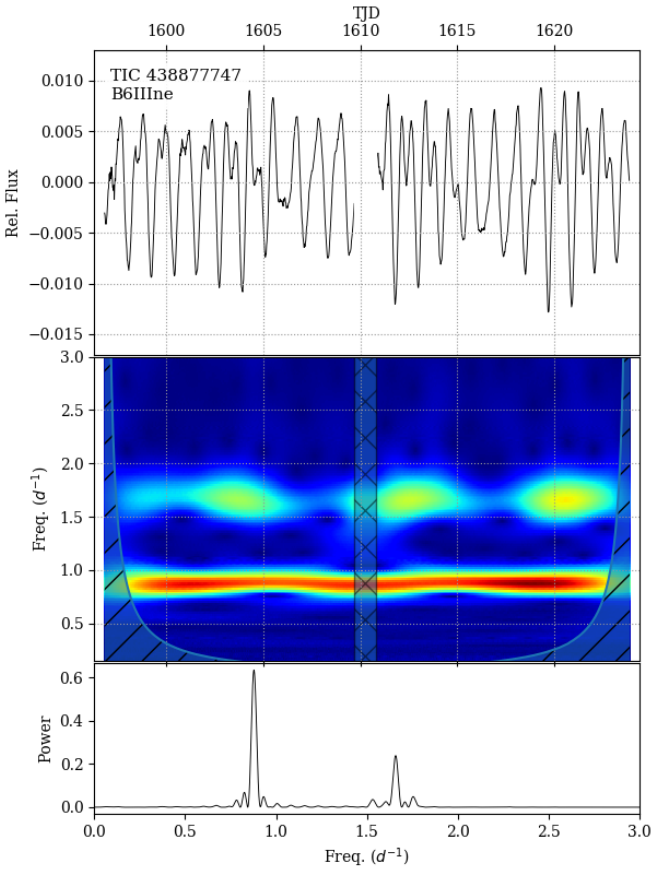

Figure 5. An example light curve and wavelet analysis for HD 112999 showing a stable frequency (near 0.9 d^{-1}) and a higher frequency group (at 1.65 d^{-1}) with a variable strength consistent with beating or a cyclical amplitude modulation.

a literature search was conducted (especially considering the historical spectral types), any available BeSS or APOGEE spectra were inspected, the SED was inspected, and any unusual features in the light curve were noted (*e.g.* indications of a short period binary). Systems deemed to be something other than a classical Be star are not considered in any of the statistics or examples in this work, and are briefly discussed in the appendix.

4.4. *Determining the center of frequency groups*

In order to determine groups of frequencies and their "center of mass", a python routine was developed to automatically identify these properties from the iterative pre-whitened frequency spectrum for each star. Broadly speaking, this routine stars with identifying the signals with the highest SNR (the "seed" signal for that group), and then moves outwards from these frequencies to identify signals that belong to the same group, while retaining information about the strength of each signal and ultimately computing the group center (with weights given in proportion to the SNR of each signal belonging to a given group). As the algorithm moves outwards from the highest SNR signals, each frequency is compared to the seed signal of the group by the equation

$$SNR(f_a) + SNR(f_b) \geq \frac{|f_a - f_b|^2}{d}, \quad (1)$$

where $SNR(f)$ is the SNR of the frequency f, f_a and f_b are the frequencies being compared and d is a weight parameter, which is calculated by

$$d = \frac{\alpha \times N_f \times I}{SNR_{\text{total}}}, \quad (2)$$

where α is a free parameter, N_f is the total number of frequencies in the spectrum, I is the interval of frequencies considered and SNR_{total} is the sum of the SNR of all N_f frequencies. If equation 1 is false for the given frequencies, the frequency is not included in the group. Otherwise, the compared frequencies are merged inside the group by replacing both with a new signal having a frequency of

$$f_{\text{new}} = \frac{f_a \times SNR(f_a) + f_b \times SNR(f_b)}{SNR(f_a) + SNR(f_b)}$$

and a SNR of

$$SNR(f_{\rm new}) = SNR(f_{\rm a}) + SNR(f_{\rm b}),$$

which is subsequently compared to the remaining signals in the spectrum. After all frequencies are analyzed in this way, the routine returns the resulting clusters of frequencies centered at the weighted average for the group, and with a characteristic strength computed from the sum of the SNRs of the original signals determined to belong to the group.

Because of the diversity of frequency spectra in the full sample, there is no single value for the α parameter that returns reliable results for all stars. Instead, this algorithm was applied to each star with three empirically determined values of α (1×10^{-3}, 5×10^{-4}, and 1×10^{-4}), where the authors then choose from these three outputs the results that best reflect the behavior of a given frequency spectrum. In practice, often all three values of α return virtually the same group information, but there are cases where a certain value of α is clearly preferable (*e.g.* in densely populated frequency spectra when groups are close together, a high value of α may erroneously merge two adjacent groups). The results from applying this algorithm are what is used to determine the location of each frequency group, and to determine the relative strengths of $g1$ and $g2$ for a given star.

5. RESULTS AND DISCUSSION FOR EACH VARIABILITY TYPE

The variability features for all Be stars in the sample were tabulated and the occurrence rates are shown in Table 1. In the following subsections, the variability types and characteristic examples are discussed. These results are discussed in a broader scope in Section 6.

5.1. *Frequency groups*

5.1.1. *Overview*

The existence of frequency groups in the power spectra is a common feature of Be stars observed from space (Walker et al. 2005a; Saio et al. 2007; Saio 2013; Kurtz et al. 2015; Baade et al. 2018; Semaan et al. 2018). 81% (361/443) of this sample shows one or more frequency groups. According to spectral type, this percentage is 87% (194/222) for early types, 93% (74/80) for mid types, and 70% (82/118) for late types. The presence of frequency groups is the most common characteristic signal seen in the Be stars of this sample. Multiple frequency groups like those seen in the majority of Be stars of this sample are not common in non-Be OB stars (*e.g.* Burssens et al. 2020; Bowman et al. 2020). Frequency groups are often a consequence of very rapid rotation in pulsators (Saio et al. 2018b; Lee & Saio 2020), and may be an important, albeit not essential, component of the Be phenomenon.

5.1.2. *Typical group configurations and relative strength*

Although there is a wide range in the location, width, number and relative strength of individual frequencies making up the group, and relative strength of the groups themselves, there are some patterns that are common when considering the whole sample. The most typical configuration includes three groups (although there may be further harmonics of these with decreasing amplitude). The lowest frequency group, $g0$, is centered at < 0.5 d^{-1} (and often much lower, around $\sim$0.05 d^{-1}). The next group, $g1$, is centered at some intermediate frequency (typically between $1 - 3$ d^{-1}), and $g2$ is located at approximately twice the frequency of $g1$. A variation of this configuration is seen when $g0$ is absent, but $g1$ and $g2$ still follow the same pattern. Figure 6 shows many examples of frequency groups, where all but panel 10 exhibit this typical configuration.

In our analysis, we recorded all cases where these typical configurations are realized (and when they are not) and the relative strength and central location of $g1$ and $g2$. No attempt was made to specify the center of $g0$ because the frequency resolution in this regime is poor owing to the short TESS observing baseline, except that, per our definition, $g0$ is centered at < 0.5 d^{-1}. For all systems with groups in the typical configuration, the central location, relative strength, and difference between the centers of $g1$ and $g2$ are shown in Figure 8

Among the systems with frequency groups, 78% (289/369) show the typical configuration with a well defined $g1$ and $g2$, with this fraction decreasing from early to mid to late spectral types (84% (162/194), 77% (57/74), and 69% (57/83), respectively, but this decrease is likely impacted by instrumental sensitivity, as amplitudes are low for later spectral types). When a frequency spectrum does include groups, but does not follow the typical configuration, there is often just one group, or, less commonly, there are multiple groups that are clearly not harmonically related (*e.g.* the second group is not located near twice the frequency of the first group). Panel 10 of Figure 6 is an example with atypical frequency groups, with a single group centered at 2.6 d^{-1} without a second group at approximately twice this frequency. It is possible that some of the stars in this sample showing an atypical group configuration are mis-classified as Be stars, but at least in the case of TIC 52748770 (HD 47160) there are many spectra in the BeSS database that confirm a weak and variable disk, consistent with its spectral classification as a classical Be star. The lack of a typical group configuration is not evidence against a given system being (or including) a classical Be star (*e.g.* Rivinius et al. 2020).

The distribution in the ratios of the central frequency of $g2$ relative to $g1$ is centered at 2.0, and is roughly symmetric (Fig. 7). Fig. 7 also compares the relative strength of $g1$ and $g2$. In 43% of systems where the typical group configuration is realized, $g1$ is stronger than $g2$, in 19% $g2$ is stronger

Table 1. Percentages showing variability classifications

	all (443)	*early* (222)	*mid* (80)	*late* (118)	*unknown* (23)
flickers	16.5% (73)	28.8% (64)	6.2% (5)	0.8% (1)	13.0% (3)
flickers + enhanced freq. groups	83.6% (61)	82.8% (53)	100.0% (5)	100.0% (1)	66.7% (2)
low freq. dominated	32.5% (144)	47.3% (105)	21.2% (17)	15.3% (18)	17.4% (4)
high freq.	14.4% (64)	14.4% (32)	17.5% (14)	13.6% (16)	8.7% (2)
very high freq.	4.5% (20)	2.3% (5)	3.8% (3)	10.2% (12)	0.0% (0)
freq. groups	83.3% (369)	87.4% (194)	92.5% (74)	70.3% (83)	78.3% (18)
typical group configuration	78.3% (289)	83.5% (162)	77.0% (57)	68.7% (57)	72.2% (13)
stochastic	27.3% (121)	35.1% (78)	15.0% (12)	21.2% (25)	26.1% (6)
isolated freqs.	33.0% (146)	25.2% (56)	37.5% (30)	45.8% (54)	26.1% (6)
harmonics of isolated freqs.	7.7% (34)	2.3% (5)	10.0% (8)	13.6% (16)	21.7% (5)

Fraction of stars showing each type of variability, according to their spectral type.

than $g1$, and in 38% $g1$ and $g2$ are of similar strength. There do not seem to be any substantial differences between early, mid, and late spectral types in these properties. Comparing the strength of $g1$ and $g2$ is somewhat subjective, but this decision is aided by the algorithm used to identify groups and their central frequency described in Sec. 4.4, which uses the sum of the signal to noise ratio of all signals determined to belong to a given group as a proxy for the group strength.

Interestingly, there are many cases where there are the typical groups $g1$ and $g2$, and a third group located at approximately twice the central value of $g2$ (and with no group near three times the central value of $g1$). Panels 7, 8, and 9 of Fig. 6 show examples of this. This is in contrast to the Be stars whose groups roughly form a harmonic series past $g1$ and $g2$ (as most clearly seen in panels 1 and 3 of Fig. 6). This may mean that in some cases, the signals that constitute $g2$ are non-sinusoidal. In typical g mode pulsators with evenly spaced frequency groups owing to a series of azimuthal orders m, the observed amplitude decreases monotonically with m due to geometric cancellation over the observed stellar disk without any "missing" harmonics (*e.g.* Saio et al. 2018a). The deviation from this pattern in some Be stars may then indicate additional complexity beyond a series of g mode groups of different m values.

5.1.3. *Group amplitude modulation and correlations between the strength of $g1$ and $g2$*

Given the short observational baseline and the often complex beating patterns that can arise in a group with more than two frequencies (see Figure 2), it is in general difficult to ascribe meaning to the apparent variability in strength of a given group and any potential correlations between the strengths of $g1$ and $g2$. There are, however, some situations where there is a fairly clear beating pattern (see Figure 5), as well as cases where the group amplitude seems to not be modulated by beating (*e.g.* Figure 4). This latter case is more interesting, as it may reflect some physical process (unlike beating) acting to enhance or suppress group strength at certain times. This is discussed further in relation to flicker evets in Section 5.2.4.

5.1.4. *Underlying physical processes and relation to rotation*

The main physical processes that can explain frequency groups in Be stars are briefly discussed below:

- g mode pulsation in rapid rotators can naturally form frequency groups, as modes with different radial orders, but the same value of l and m will oscillate at similar but slightly different frequencies. For sectoral g modes (*i.e.* $l = |m|$ and no latitudinal nodal lines exist, which are common in Be stars, Rivinius et al. 2003; Maintz et al. 2003; Neiner et al. 2012a), the frequency in the inertial (observational) frame is proportional to $|m|$ and the first group is generally found above the rotation frequency by about 20% (Cameron et al. 2008; Saio et al. 2018a,b; Semaan et al. 2018). Detailed modeling applied to the case of a rapidly rotating γ dor star observed with Kepler (KIC 5608334), which displays a series of frequency groups not dissimilar to those seen in Be stars, demonstrates this situation (Saio et al. 2018a).

- r modes in moderate to rapidly rotating stars also form frequency groups, but generally centered at different frequencies compared to g mode groups (Saio et al. 2018b). The strongest of these r mode groups ($|m| = 1$) is located at slightly below the rotational frequency, with further groups becoming weaker in observed amplitude with increasing $|m|$, and located slightly below $|m| \times \nu_{rot}$.

- Variability in the circumstellar environment, especially during active mass ejection, can cause frequency

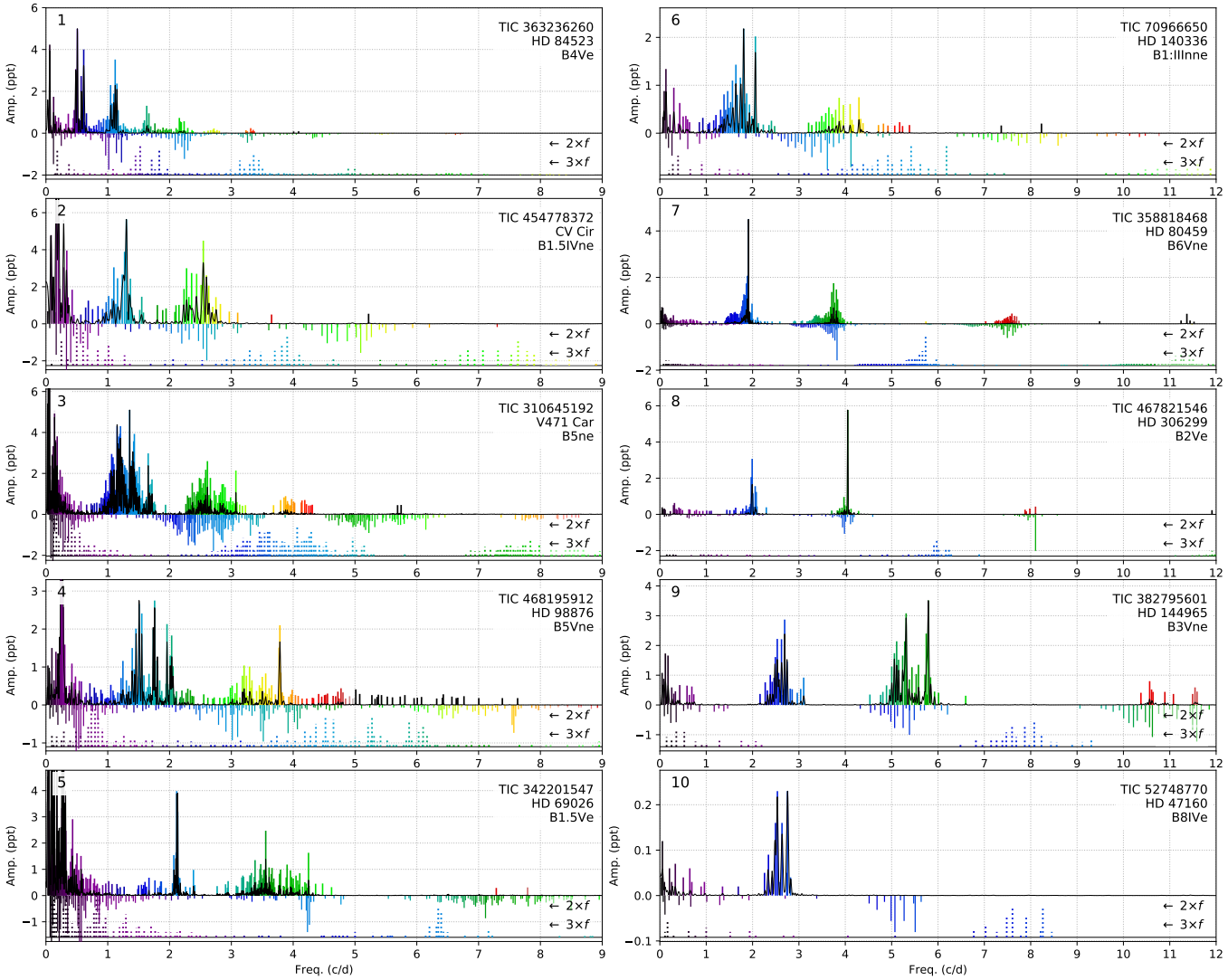

Figure 6. A selection of frequency spectra showing various permutations of group configurations and morphology. Solid colored vertical lines are the signals recovered with iterative pre-whitening, and the solid black line is the Lomb-Scargle periodogram without any pre-whitening normalized to the highest amplitude at $f > 0.33$ d^{-1}. The inverted solid lines show the same frequencies multiplied by two, and below that, the dashed lines show the frequencies multiplied by three to aid in visualizing the locations of the first and second harmonics of the recovered signals. *1:* Closely spaced, narrow groups monotonically decreasing in strength. *2:* $g1$ and $g2$ have similar strengths, without further harmonics. *3:* Wider groups, with signals corresponding to the second harmonic of $g1$, but without significant signals corresponding to the first harmonic of $g2$ (or the third harmonic of $g1$). *4:* $g1$ and $g2$ are wide, and the region beyond $g2$ is populated with signals that form a "continuum" corresponding to harmonics of signals in $g1$ and $g2$. *5:* $g1$ is narrow and dominated by a single signal, and $g2$ is relatively wide and centered at a frequency less than $2 \times g1$. *6:* $g2$ is centered at greater than $2 \times g1$, and there are also signals located in the region occupied by the second harmonic of $g1$. *7:* $g1$ and $g2$ are narrow and mirror each other in structure, but there are only signals that correspond to $2 \times g2$ and not $3 \times g1$. *8:* Even more narrow groups, with $g2$ being the stronger of the two main groups. *9:* Widely separated groups, where $g2$ is stronger than $g1$, and with power located in the region corresponding to $2 \times g2$ and not $3 \times g1$. *10:* Only one frequency group exists.

groups near and slightly below the rotational frequency, and also generate harmonics (Štefl et al. 1998; Baade et al. 2016). The characteristic frequencies of this phenomenon is dictated by the orbital timescale close to the star, which depends on the orbital radius of the recently ejected material (which generally evolves with time).

- Balona & Ozuyar (2020) argue that rotation is the primary cause of the periodic signals and frequency groups in Be stars from a large sample of TESS light curves, many of which overlap with the sample of this work. The proposed mechanism is small-scale magnetic fields that force material to co-rotate with the star, which can obscure the stellar surface as a line of sight

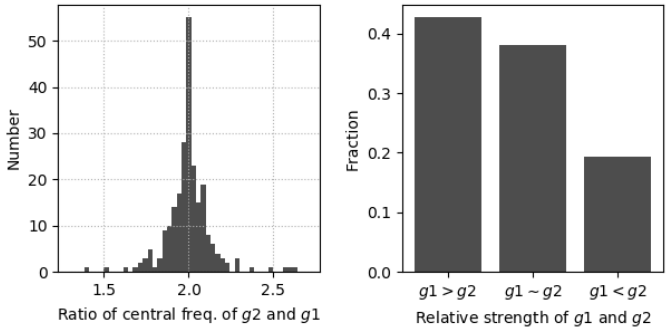

Figure 7. *Left*: Histogram of the ratio of the central frequency of $g2$ and $g1$. *Right*: Comparison of the relative strength of $g1$ and $g2$.

effect, leading to periodic signals at (and near) the rotational frequency and its harmonics.

5.1.5. *Interpreting frequency groups and their relevance in the Be phenomenon*

Frequency groups in classical Be stars are clearly complex in their nature. The majority of Be stars do exhibit two or more frequency groups, suggesting they are an important aspect of the Be phenomenon. However, a significant fraction of these systems show only one or zero frequency groups, suggesting that two or more frequency groups, at least in some systems, is not a necessary observable condition for the ejection of matter. This is contingent on the noise level (perhaps there are low amplitude frequency groups below the detection threshold), and it is also sometimes observed that the strength of groups and/or their most prominent frequencies can significantly vary over time (Smith et al. 2006; Borre et al. 2020; Labadie-Bartz & Carciofi 2020, Labadie-Bartz et al. 2020, subm.), so that the lack of observed groups at the time when a given star is observed by TESS does not necessarily mean that groups have not existed in the past (or will not become more prominent in the future).

Semaan et al. (2018) find a relationship between the spacing of groups in Be stars and their spectroscopically-measured rotational frequency: $\delta f = (1.24 \pm 0.28) \times f_{rot}$, where δf is the difference between adjacent groups ($g2 - g1$ in our notation). This linear relationship seems to be in agreement with other works that attempt to explain the frequency groups (understood as either g and/or r modes) in Be stars observed with MOST (Cameron et al. 2008; Saio et al. 2007). This relationship also holds true for the rapidly rotating A-type γ dor pulsator observed by Kepler (KIC 5608334 Saio et al. 2018b), where the $f_{rot} \approx 2.2$ d^{-1}, and the spacing between the prograde sectoral g-mode frequency groups of $-m = 1, 2, 3, 4$ is $\delta f \approx 2.8$ d^{-1}.

In typical g-mode pulsators with evenly spaced frequency groups owing to a series of azimuthal orders m, the observed amplitude decreases monotonically due to geometric cancellation over the observed stellar disk. Only some Be stars follow this pattern, suggesting the nature of frequency groups may be more mixed compared to the more well understood cases of γ dor pulsators.

Saio et al. (2018b) model r and g modes in the Kepler Be star KIC 6954726 (one of the three Kepler Be stars studied in Rivinius et al. 2016), and find that r modes can explain some of the features in the frequency spectrum (mainly, the central part of the first frequency group, $g1$ in our notation) and that g modes do not seem to make a substantial contribution. However, the frequency spectrum is more complex than can be explained by r modes (plus a rotational frequency) alone, and it is likely that circumstellar activity contributes (as suggested by Rivinius et al. 2016). Further, r modes are necessarily retrograde in rapid rotators, meaning they can not substantially contribute to the mass ejection mechanism and the net outward flux of angular momentum. This is in contrast to prograde g modes, which can transport angular momentum outward and locally enhance the velocity field of material at the stellar surface, lowering the barrier for mass ejection.

As pointed out in Saio et al. (2018b), outbursts in Be stars likely disrupt the rotational flow on the stellar surface. Outbursts, or rather the resulting surface flow disruption, then may trigger r modes. This insight further complicates the interpretation of frequency groups in active Be stars, since both r modes and frequencies arising from an inhomogeneous circumstellar environment (Štefl frequencies) are expected at frequencies slightly below that of the rotation of the star. This challenge can be ameliorated with spectroscopic observations, where the circumstellar contribution is more easily identified.

5.2. *Flickers*

5.2.1. *Background and overview*

Outbursts (discrete episodes of mass ejection) are a well-known and common feature of Be stars which manifest in photometry as an increase in brightness as the growing quantity of circumstellar material emits and re-processes stellar light (Sigut & Patel 2013; Haubois et al. 2012; Labadie-Bartz et al. 2018). In the case of systems viewed at high inclination angles ($i \gtrsim 75$ degrees), the growth of a disk instead causes a net dimming, as the relatively cool circumstellar material obscures the stellar photosphere. The timescales of outbursts range from days to many years or even longer (Labadie-Bartz et al. 2018; Rímulo et al. 2018; Bernhard et al. 2018; Ghoreyshi et al. 2018). The term "flicker" can be used to describe mass ejection events with short timescales (days to weeks, Keller et al. 2002). With the relatively short baseline of TESS light curves, it is only possible to probe these flickers on short timescales. Due mostly to a lack of a sufficiently large sample with high-precision near-continuous photometry, flickers with timescales of days have so far been poorly studied.

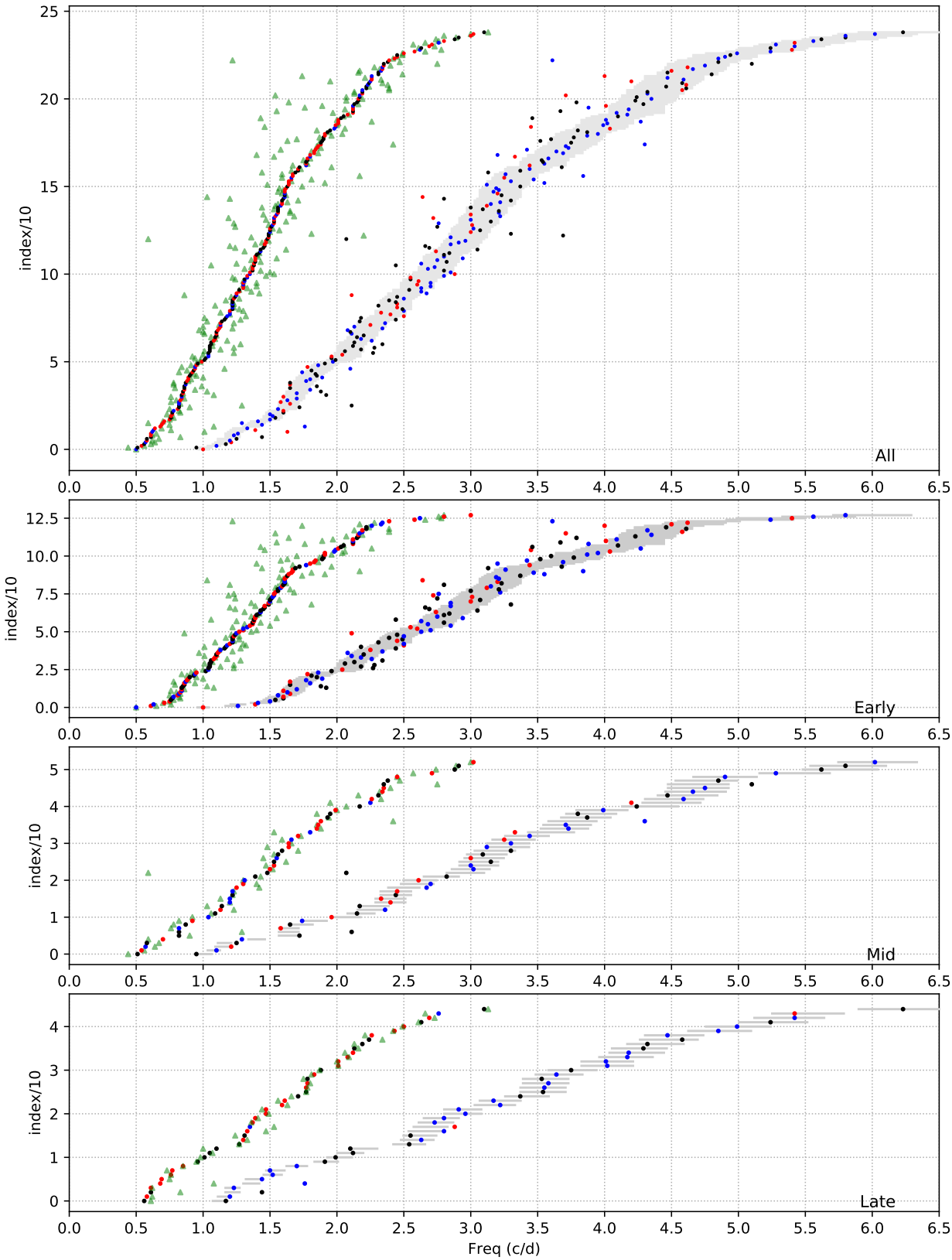

Figure 8. The center of the two main frequency groups are shown for each system with a typical frequency group configuration. The stars are ordered according to the location of $g1$, increasing upwards. Black dots are used when the strength of the two groups are similar, and red (blue) dots indicate when one group is stronger (weaker). The grey lines are centered at $2 \times g1 \pm 5\%$. Green triangles mark $g2 - g1$.

As exemplified in the Be star HD 49330 observed with CoRoT (Huat et al. 2009), a typical flicker event can be broken up into four phases – the relative quiescence phase (where the light curve is flat), the precursor phase (where the brightness gradually and mildly decreases), the outburst phase (where the brightness increases), and a relaxation phase (where the brightness returns towards the baseline level). These phases also have spectroscopic counterparts (*e.g.* Rivinius et al. 1998a). Precursor phases are not always seen.

5.2.2. *Main results from TESS*

Flickers were found in 17% (73/443) of the sample. There is a strong dependence on spectral type, with 29% (64/222) of early systems, and 6% (5/80) and 1% (1/118) of mid- and late-type systems showing flickers. This is consistent with other observational studies that find early Be stars to be significantly more variable and active, and with relatively large disk densities (and therefore higher amplitude observables, Vieira et al. 2017; Labadie-Bartz et al. 2018).

In this work, only flickers inducing a net brightening are recorded. Shell stars ($i \gtrsim 75$) that eject mass instead have flickers that manifest in photometry as a net dimming. These dimming flickers are relatively difficult to confirm with photometry alone on the short timescales of TESS observations, largely because of the relatively small amplitude and naturally longer timescale of the change in optical continuum flux compared to equivalent events viewed at lower inclination angles (Haubois et al. 2012). Nevertheless, there are a few instances in this sample where dimming flickers are apparent. Figure 11 shows an example of this.

Systems viewed at an inclination angle of $i \sim 70$ degrees may exhibit no detectable change in their optical flux associated with the growth or dissipation of a disk – single-band photometry is largely blind to disk events at this intermediate inclination angle (Haubois et al. 2012). Some Be stars build up disks over timescales much longer than a TESS observing sector (*e.g.* Rímulo et al. 2018; Labadie-Bartz et al. 2017), where the rate of change in brightness is gradual and difficult to detect in TESS. Mass loss happening on top of a strong pre-existing disk may impart little to no photometric excess, as Be disks can become saturated in certain observables, including visual continuum flux (Haubois et al. 2012). Weak mass loss events can occur, which may still contribute to the disk mass budget, but without a significant detectable photometric signature. For these (and possibly other) reasons, the incidence rate of flickers in our sample is underestimated, and it is not the case that the lack of flickers in a given system implies the absence of ongoing mass ejection.

5.2.3. *Photometric flickers as tracers of mass ejection*

Even photometric flickers with very short duration and small amplitude can still be interpreted as mass ejection episodes. Figure 9 demonstrates an example where the TESS brightness and Hα line profile evolve together during such an event for the Be star HD 194779, which was observed multiple times spectroscopically over the TESS observing baseline. In this system, the Hα line indicates a transition from a disk-less to a disk-possessing state. This transition unambiguously indicates the ejection of material from the star into the circumstellar environment, which coincides with a flicker as seen in the TESS photometry. Although this system was observed in TESS Cycle 2, and is thus not included in the present sample, it serves to illustrate the connection between a photometric flicker and the ejection of stellar material even in this case where the amplitude and duration are small. A spectroscopic campaign including HD 194779 and many other Be stars contemporaneous with TESS observations is ongoing and will be the subject of forthcoming works, with preliminary results reinforcing the interpretation of photometric flickers as mass ejection events.

5.2.4. *Flickers and frequency groups*

Other works have presented evidence of the frequency spectrum changing before, during, and after outbursts (*e.g.* Huat et al. 2009; Baade et al. 2018; Semaan et al. 2018). This is also seen in the majority of flickering Be stars in this sample, as there are many cases where flickers coincide with the emergence or enhancement of frequency groups. About 84% (61/73) of stars with flickers show this behavior. Under the interpretation that flickers correspond to mass ejection events, there is some ambiguity in interpreting the enhancement of frequency groups in these instances. Frequencies about 10% lower than the dominant pulsation frequency were first discovered in the line profiles of Be stars actively ejecting material (and later seen in photometry of active Be stars), with the preferred interpretation being that they arise in the circumstellar environment due to an inhomogeneous distribution of recently ejected material orbiting the star (Štefl frequencies; Štefl et al. 1998; Baade et al. 2016). The enhancement of the overall strength of a frequency group during times of outburst may then be related to increased pulsational amplitude and/or circumstellar variability. Circumstellar signals are expected to be stronger in systems viewed at higher inclination angles

A few examples of systems with flickers are shown in Figure 10, along with a wavelet analysis showing how the strength of the frequency groups evolves. One or more frequency groups is often, but not always, enhanced during or near a flicker. In systems with typical group configurations with flickers, it is more common for $g2$ to be more strongly variable than $g1$ (as is seen in all but the second panel in Figure 10). All systems exhibiting flickers also have one or more frequency groups.

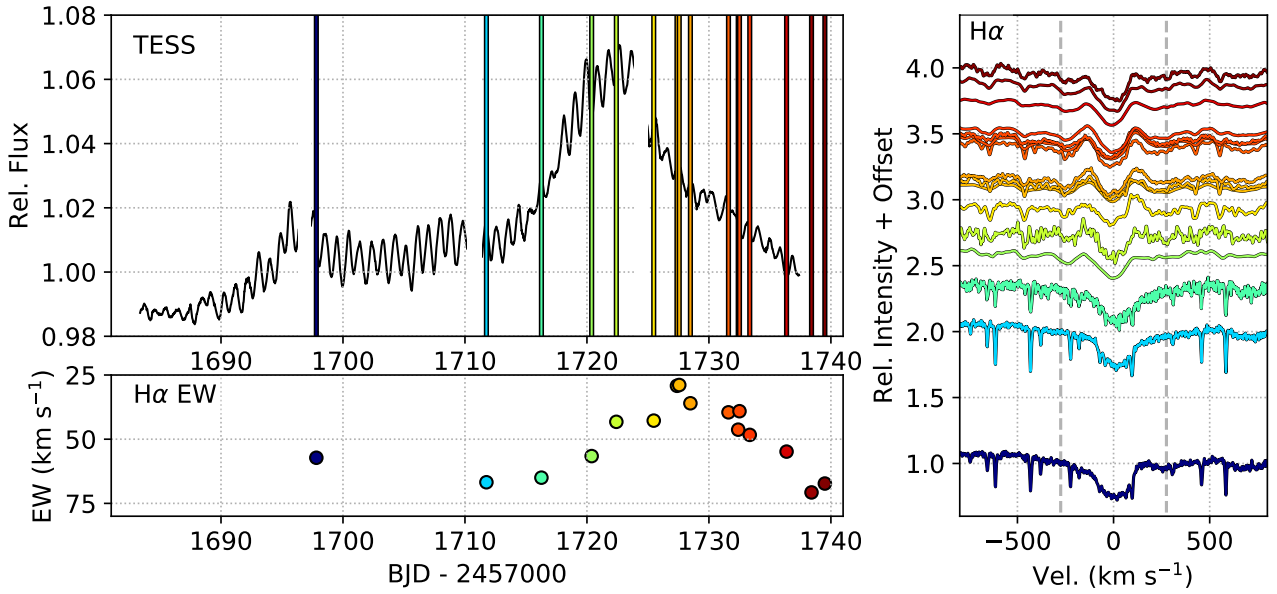

Figure 9. An example of a star with a typical flicker that was monitored spectroscopically during TESS observations. A portion of the TESS light curve is shown, along with the Hα line from the spectroscopic observations. The vertical colored lines indicate the spectroscopic epochs, with the corresponding line profiles in the right panel (time increasing upward). Hα emission begins to appear near TJD = 1720, indicating that material is being ejected into the circumstellar environment. Line asymmetries at the first two spectra may also indicate mass loss, albeit at too small rate to support disk formation. The Hα equivalent width (EW) is plotted in the bottom panel.

The temporary in-phase superposition of two or more modes in a frequency group has been in some instances found to correspond to mass ejection episodes (Rivinius et al. 1998b; Baade et al. 2016, 2018; Baade & Rivinius 2020). In some of these cases, the resultant amplitude is greater than the sum of the base mode amplitudes, perhaps indicating nonlinear amplification (as opposed to beating). The enhancement in frequency group strength seen to commonly coincide with flickers in the TESS data may reflect this – *i.e.* non-linear amplification (or in the simplest case, linear beating) in the amplitude of frequency groups may be triggering some of the flickers.

5.2.5. *Comparison to other studies*

Flickers on the short timescales that are seen in TESS data have been captured in other Be stars with space photometry. In Kepler data for 3 Be stars, flickers are found in two systems with timescales of about 10 – 50 days (Rivinius et al. 2016). Using data from CoRoT, Semaan et al. (2018) analyzed light curves for 15 Be stars, highlighting 6 with flicker events with total durations between about 10 – 60 days. However, until this work, there has been a lack of analysis of a large set of space photometery for Be stars. The large dataset provided by TESS opens a window into studying these events in individual systems, but perhaps more importantly allows for the study of larger numbers of systems showing these events than has been possible prior to the launch of TESS, providing insight into the types of systems showing small-scale flickers and how frequently they occur.

5.3. *High and Very High Frequencies*

5.3.1. *Main results for high frequencies* ($6 < f < 15\ d^{-1}$)

A subset of the sample (14%, 64/443) has high frequency signals ($6 < f < 15$ d^{-1}) that are not simply harmonics of the typical frequency groups (or isolated signals at lower frequencies), but are rather individual frequencies (or they can exist in groups, but with a different morphology or configuration than the typical lower frequency groups). It should be kept in mind, however, that the short baseline of TESS implies a frequency resolution of ≈ 0.04 d^{-1}, so it is possible that what is here detected as single frequencies might be two or more unresolved frequencies.

β Cephei stars are early B-type (roughly B0 – B2.5) that pulsate in p modes with typical frequencies between 3 – 12 d^{-1} (Stankov & Handler 2005). While Be stars most typically show low frequency pulsation similar to the SPB stars (De Cat 2002), some classical Be stars are also observed to have β Cephei pulsation (*e.g.* Nazé et al. 2020; Huat et al. 2009; Walker et al. 2005b). It is likely that some fraction of the Be stars that show these high frequency signals in TESS also belong to the class of Be stars that are SPB/β Cephei hybrid pulsators.

However, signals in the traditional β Cephei regime are not necessarily p modes, because a pulsational signal in the SPB regime in the co-rotating frame can be pushed to higher observed frequencies in rapidly rotating stars via the equation $f_{\rm obs} = f_{\rm corot} - m\,\Omega$, where Ω is the rotational frequency of the star, and m is the azimuthal order of the pulsation mode (be-

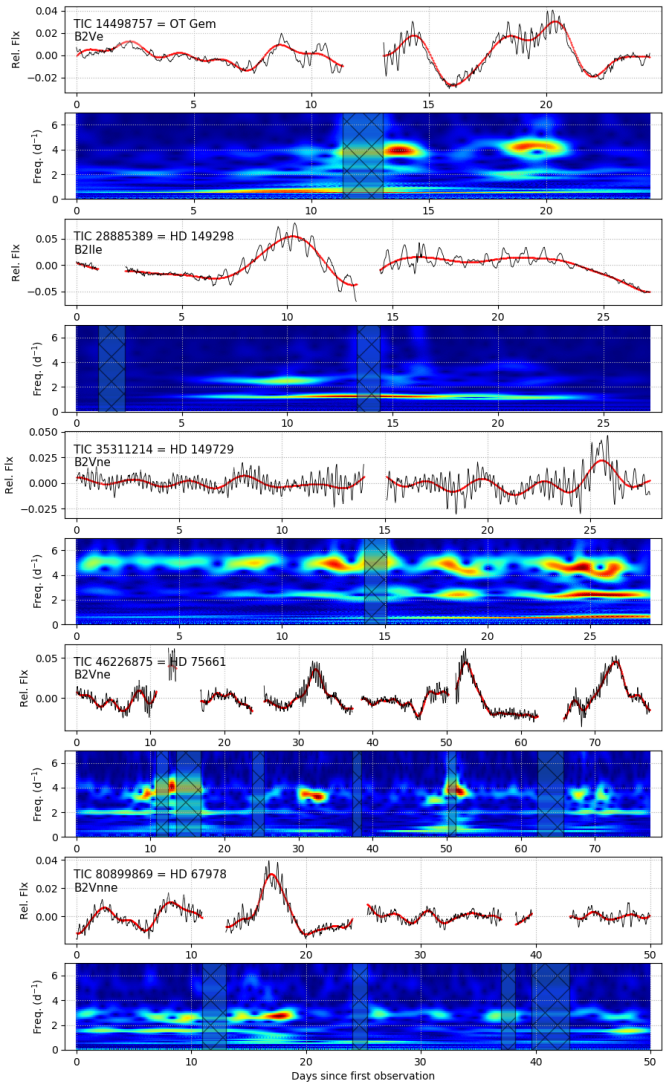

Figure 10. Examples of systems with flickers. Below each light curve is the wavelet plot showing the evolution of the frequency spectrum over time after subtracting the low frequency signals (the red curve).

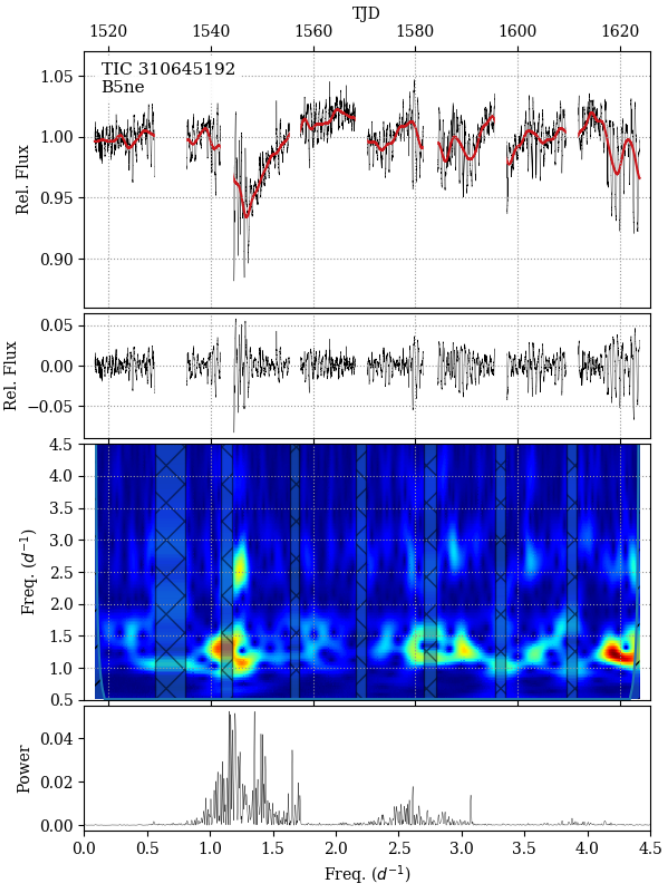

Figure 11. An example of a system (TIC 310645192) that shows dimming flickers (most apparent at TJD = 1540).

ing negative for prograde modes, and positive for retrograde modes). However, such a situation usually appears in the frequency spectrum as a harmonic series of groups (*e.g.* panels 7 and 9 of Figure 6), and these signals would therefore not be considered as (isolated) high frequencies. There is also the possibility of combination frequencies as described in Kurtz et al. (2015), which may be an important ingredient in the observed frequency spectra.

Perhaps surprisingly, the presence of high frequency signals is not limited to early type stars. This is counter-intuitive if these signals reflect β Cephei pulsation, since the β Cephei phenomenon (*i.e.* p modes excited by the κ mechanism) is restricted to early B-type stars. We find high frequency signals in 14% (32/222) of early-type, 18% (14/80) of mid-type, and 14% (16/118) of late-type stars.

5.3.2. *Main results for very high frequencies ($f > 15\ d^{-1}$)*

Very high frequencies are uncommon. 5% (20/443) of this sample have signals beyond the typical β Cephei regime with frequencies greater than 15 d^{-1}. The highest frequency signals detected are near 75 d^{-1} in the system TIC 427400331 = HD 290662. Signals at the lower end of this very high frequency regime may be typical p mode pulsation shifted to higher observed frequencies due to rapid rotation, as is suggested for the signals at 17.27 and 19.31 d^{-1} in the Oe star ζ Ophiuchi (Walker et al. 2005b). Or, in some cases, combination frequencies (and harmonics, which are explicitly not included in this aspect of this work) can produce signals at very high frequencies, and therefore some very high frequency signals (mostly towards the lower end of this range) may not be independent, but rather a sum of two lower frequency signals (or perhaps a more complex combination, Kurtz et al. 2015; Burssens et al. 2020).

However, towards the higher end of these very high frequencies, it is not plausible that they arise in a classical

Be star. Instead, these may indicate the presence of a stellar companion pulsating at these relatively high frequencies. This may be supported by the higher incidence of very high frequency signals in later spectral types (2% (5/223), 4% (3/80), and 10% (12/120) in early, mid, and late types, respectively) which is an expected trend if these signals do indeed indicate a companion since the contrast ratio between the Be star and a hypothetical companion will be less severe for Be stars of later spectral type.

Figure 12 shows the frequency spectra of a selection of systems with high and very high frequency signals. For stars with 2-minute cadence light curves, frequencies out to 360 d^{-1} can be probed, as opposed to 24 d^{-1} for 30-minute cadence data. This limits our ability to detect the highest frequency signals to the ∼65% of systems with 2-minute cadence data, and so the percentage of systems in which very high frequencies are detected is likely slightly underestimated. Among the 20 objects with frequencies > 15 d^{-1}, only 3 had signals above 24 d^{-1}.

5.3.3. *Binarity and composite frequency spectra*

Binarity is common in the massive star population, with the majority of B-type stars being members of a multiple star system (*e.g.* Kouwenhoven et al. 2007). Oudmaijer & Parr (2010) find essentially the same binary fraction and properties when comparing Be vs. B stars. While the binary fraction of Be stars is poorly constrained (due largely to their broad absorption lines and high luminosity), many Be stars are known to have a binary companion. The frequency spectra of binary systems will then contain signals from two (or more) sources if they are variable. In fact, the prototype of the β Cephei class, β Cephei, is a binary with a slowly rotating β Cephei primary and a rapidly rotating mid B-type classical Be star (Wheelwright et al. 2009). Often in Be binaries, the companion to the Be star is an evolved object, such as an sdOB star (Gies et al. 1998; Chojnowski et al. 2018; Wang et al. 2018, and references therein), a neutron star (*i.e.* a Be X-ray binary system; Ziolkowski 2002), or even a black hole (Casares et al. 2014). Even though a Be companion need not be significantly evolved, a recent study (Bodensteiner et al. 2020) found no firm evidence for main sequence companions around Be stars (note, however, that low-mass main sequence companions are difficult to detect because the total flux of the system tends to be dominated by the Be star, and that this study does not include the aforementioned β Cephei system). Some unknown fraction of this TESS sample of Be stars are in binaries. It is therefore possible (and in some cases, likely) that some of the high and very high frequency signals detected in the TESS data arise not from the Be star, but from a companion. Compounded by the large pixel size of TESS, it is not possible to resolve these cases and determine which signals originate in the Be star from just TESS photometry.

5.3.4. *Potential pulsating companions*

Some examples of stars with pulsation at greater than 15 d^{-1} include the main sequence A-type roAp stars with periods between 6 – 20 minutes ($f \sim 72 - 240$ d^{-1}) and amplitudes of a few mmag (Kurtz 1982), and the (usually, but not always, main sequence A/F type) δ Scuti stars with typical periods between 0.02 - 0.25 d ($f \sim 4 - 50$ d^{-1}) and typical amplitudes between 3 – 10 mmag, but sometimes up to and in excess of 0.3 mag (the high amplitude δ scuti stars; Breger 2000; Garg et al. 2010).

Perhaps most relevant for Be star systems are those with hot subdwarf (sdOB) companions, where at some earlier time the initially more massive star expanded and donated mass and angular momentum to the present-day Be star, shedding its envelope and leaving behind its core (the sdOB star). Such Be+sdOB systems typically have (near) circular orbits with periods of roughly 100 days (*e.g.* Bozic et al. 1995; Bjorkman et al. 2002; Chojnowski et al. 2018; Peters et al. 2016). sdOB stars are also known to pulsate in this high to very high frequency regime. In sdOB stars, p-mode pulsations typically have periods between 2 – 10 minutes ($f \sim 144 - 720$ d^{-1}), and amplitudes of about 1% (∼10 mmag, Kilkenny et al. 1997), and g modes oscillate with periods between about 45 minutes – 2 hours ($f \sim 12 - 32$ d^{-1}) and amplitudes typically between 0.1 – 0.5 % (∼1 – 5 mmag, Green et al. 2003; Kawaler et al. 2010). However, in some cases the amplitudes can be much larger, and an sdOB star can pulsate in both p and g modes. For example, the sdO star PG 1605+072 shows over 55 modes, the strongest of which has a period of 8.03 minutes ($f = 180$ d^{-1}) and an amplitude of over 50 mmag (about 5%, Pereira & Lopes 2004). Sahoo et al. (2020) analyze TESS data for three hot subdwarfs, finding frequencies between about 9 – 300 d^{-1}, with most of the signals being between about 15 – 30 d^{-1}. These signals have typical amplitudes of less than 1 ppt.

In most cases, the Be star dominates the visible flux in Be binary systems. This can severely dilute any signals originating in a companion, to the point of being undetectable even with space photometry. However, there are many possible configurations where such a signal in a companion can rise above the detection threshold despite the contaminating flux from the Be star. For example, in the well known B0.5Ve+sdO binary ϕ Per (Gies et al. 1998; Poeckert 1981), the sdO star contributes approximately 3% of the total visible flux (Mourard et al. 2015). If the sdO star were to pulsate with an amplitude of 50 mmag (like PG 1605+072), this signal would be diluted down to an amplitude of ∼1.5 mmag, which is easily detectable in space photometry provided the observing cadence is such that the frequency of the signal is

not beyond the Nyquist limit and the exposure time is sufficiently short. The flux ratio between the Be star and its companion can be even lower for later type Be primaries, such as the B5e primary in the 7 Vul binary system (which is suspected to have an sdOB companion; Vennes et al. 2011), although it should be noted that most confirmed Be+sdOB binaries have primaries with spectral types between B0 – B3 (Wang et al. 2018). 2-minute cadence TESS light curves are much better suited to this task (with a Nyquist limit of 360 d^{-1}) compared to the 30-minute light curves (Nyquist limit of 24 d^{-1}).

These systems with very high frequencies are therefore good candidates for further study to search for evidence of binarity. This can be done through radial velocity monitoring of the Be star and its disk (Miroshnichenko et al. 2002; Bjorkman et al. 2002), direct detection of spectral features (and their radial velocity) of a companion (Wang et al. 2018; Chojnowski et al. 2018), modeling of the radial structure of the Be star disk to infer truncation from a binary companion (Klement et al. 2019), and to observe the radial and azimuthal structure of the disk to detect density waves that propagate at the orbital period, which are caused by tidal forces from a binary companion (Panoglou et al. 2016, 2018, 2019; Chojnowski et al. 2018; Cyr et al. 2020). Direct interferometric detection may also be possible.

This is an important topic because the binary fraction of Be stars is poorly constrained, and one of the proposed evolutionary channels by which a Be star achieves its near-critical rotation is through binary interaction (Pols et al. 1991; de Mink et al. 2013), as opposed to, or in addition to, outward angular momentum transfer from a contracting core in a single stellar evolution scenario (Ekström et al. 2008; Granada et al. 2013). All systems in which we detect very high frequencies are discussed in the appendix.

5.4. *Stochastic Variability*

5.4.1. *Overview and main results from TESS*

Stochastic variability is sometimes a prominent feature in the frequency spectra of Be stars, as has been pointed out for some Be stars observed from space (e.g. η Cen, Baade et al. 2016, where the star is apparently nearly continually losing mass). 27% (121/443) of this sample has stochastic variability as a prominent feature. Stochastic variability is prominent among early (35%, 78/222), mid (15%, 12/80) and late (21%; 25/120) spectral types, with amplitudes generally being highest in early type stars. Figure 13 shows 6 systems where stochastic variability is a prominent feature.

In this work, the designation of stochastic variability is applied qualitatively. An important difference between this work and the work and terminology of, *e.g.*, Bowman et al. (2019, 2020), is that we consider a system to show stochastic variability only if it is obviously a dominant aspect of its light curve and frequency spectrum (viewed in a linear scale). Otherwise, without more in-depth analysis, this label becomes meaningless as virtually every star in this sample is expected to have some degree of stochastic variability (*i.e.* astrophysical correlated red noise) as it is defined in other works like Bowman et al. (2019, 2020). A proper analysis and parameterization of the stochastic low frequency excess of the TESS Be star sample can and should be undertaken and compared to the results for the more slowly rotating OB star sample of (Bowman et al. 2020).

5.4.2. *Underlying mechanism(s) and relevance to the Be phenomenon*

Stochastic variability is a ubiquitous feature of OB stars (*e.g.* Bowman et al. 2019, 2020), with a wide range in amplitude and characteristic timescale. There are many physical processes that can plausibly give rise stochastic variability in classical Be stars, including inhomogeneities in the stellar surface or wind combined with rotation (Moffat 2008; Aerts et al. 2018; Simón-Díaz et al. 2018), sub-surface convection layers (Cantiello et al. 2009, 2011; Cantiello & Braithwaite 2011, 2019), and internal gravity waves generated at the interface between the convective core and the radiative envelope, which propagate outwards (Rogers et al. 2013; Horst et al. 2020; Edelmann et al. 2019; Bowman et al. 2019). Although stochastic variability does not contain any coherent periodic signals, there is still valuable diagnostic potential in the profile and amplitude of the frequency spectrum of these stochastic signals. For example, Bowman et al. (2020) analyzed TESS data for 70 OB stars with TESS, concluding that there is strong evidence for internal gravity waves by comparing measurements of the stochastic frequency spectrum to models of wave propagation in stellar interiors which originate at interface of the convective core and radiative envelope.

These internal gravity waves may be an important aspect of Be stars, since they are efficient at transporting angular momentum from the stellar interior outward (Rogers et al. 2013; Edelmann et al. 2019). While it is beyond the scope of this work to quantitatively analyze the stochastic variability seen in the TESS Be star sample, it is important to note that these features, although appearing random and incoherent, can still be used as a diagnostic to infer the physical origin(s) of the signals.

Furthermore, internal gravity waves can drive g mode pulsation in Be star envelopes. This is especially important in early type Be stars, which are generally too hot for the κ mechanism to excite g mode pulsations (Dziembowski et al. 1993; Neiner et al. 2012b, 2020). However, even in the hottest Be stars the κ mechanism may still act in some limited capacity to drive g modes if certain conditions are met (Pamyatnykh 1999; Neiner et al. 2012b), such as enhanced metallicity or if the star is evolved to near the terminal age

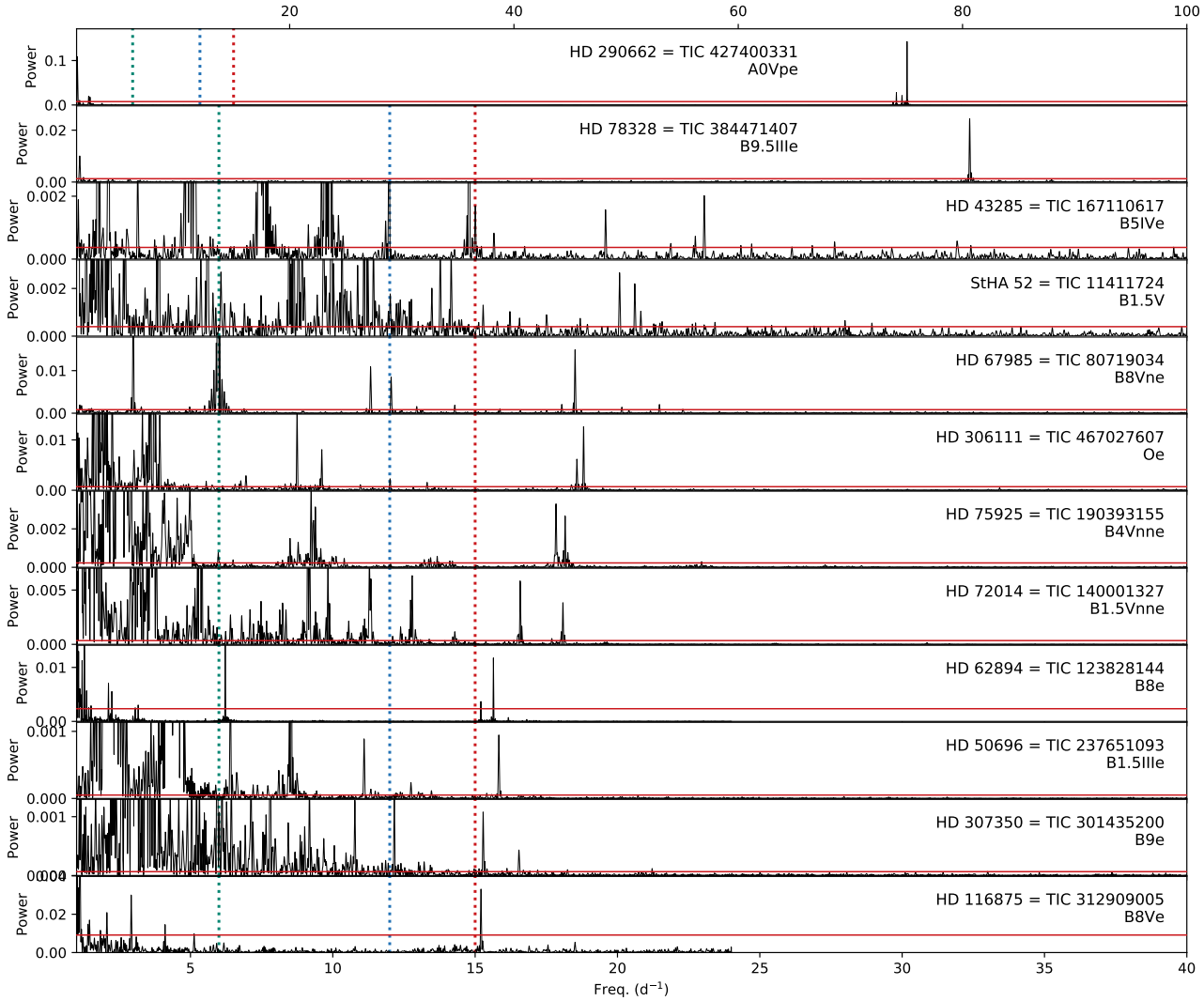

Figure 12. Shows frequency spectra of systems with high and very high frequencies. Vertical dotted lines are at 6, 12, and 15 d^{-1} for reference. In the top panel the x-axis extends to 100 d^{-1}, while the remainder share the same axis, out to 40 d^{-1}.

main sequence (TAMS), but this alone cannot explain the observed distribution of frequency groups among the earliest stars in this sample.

Since virtually all of the Be stars with frequency groups have $g1$ in the traditional low frequency g mode regime (including the early spectral types, Fig. 8), the excitation of these modes by internal gravity waves may even be fundamental to the Be phenomenon in these systems. As outlined in Neiner et al. (2020), internal gravity waves can serve the dual purpose of transporting angular momentum to the envelope (causing it to spin up and lowering the barrier to mass ejection) and can also excite groups of g mode pulsation, where the activity and processes in the surface layers may then meet the conditions required to trigger an outburst whereby mass and angular momentum is transported to the disk and ultimately out of the system.

5.5. *Low frequency dominated light curves*

The light curves of 34% (151/443) of this sample are dominated by low frequency variability ($f < 0.5$ d^{-1}), which may or may not be periodic or cyclic in nature. Like most other types of variability, the light curves of early type stars are more likely to display this behavior (48%; 106/223) compared to mid (20%; 16/80) and late (19%; 23/120) types. Flickers stand out as the most remarkable type of behavior that causes a light curve to be dominated by low frequency signals, and in these cases the low frequencies are (at least in part) tied to occasional episodes of mass ejection.

However, not all systems with low frequency signals exhibit flickers, and systems in which low frequencies dominate are not necessarily ejecting mass during TESS observations. These slow signals can reflect pulsation – in particular the non-linear coupling of two or more pulsation modes, as

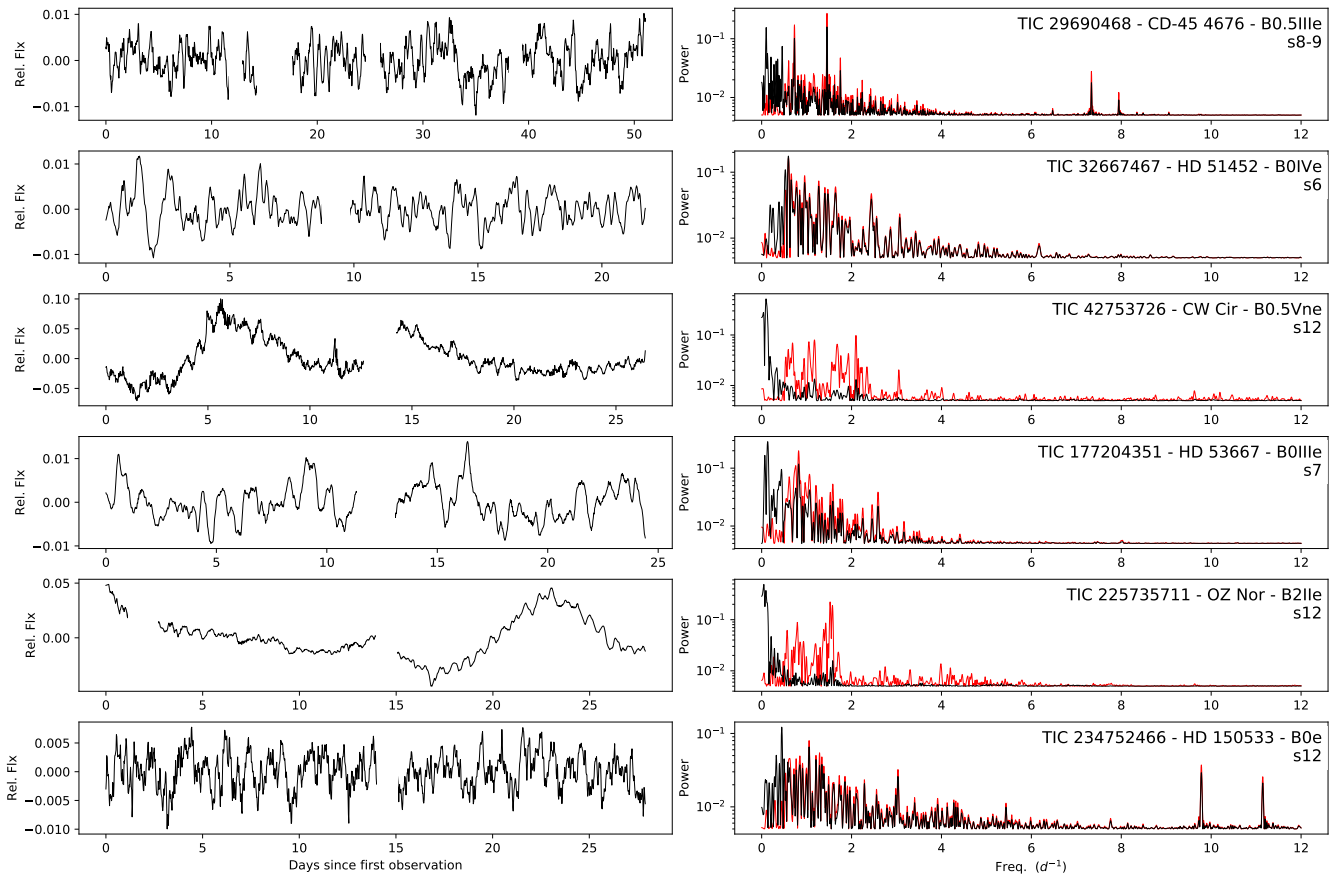

Figure 13. Light curves (left) and frequency spectra (right) of a few example systems exhibiting stochastic variability. In the frequency spectra plots, the black curve is computed from the raw data (shown in the light curve plots), and the red curve is computed after removing signals with frequencies below 0.5 d^{-1}.

a simple beating pattern of two frequencies will not produce power at their beating period in a frequency spectrum.

In the notation of this study and other works, often multiple signals form a low frequency group ($g0$) below 0.5 d^{-1}. In space photometry with longer observational baselines (*e.g.* BRITE, CoRoT, Kepler, and SMEI), it is sometimes found that one or more of the signals in $g0$ are related to prominent signals in $g1$ through difference frequencies. That is, a signal in $g0$ is found at the difference between two signals in $g1$. Since there are often many frequencies in $g1$, $g0$ can be populated by multiple difference frequencies. Unfortunately, the TESS observational baseline is usually too short to confidently measure the position of signals in $g0$, so in the present work no attempt is made to relate the frequencies in $g0$ to those in $g1$.

5.6. *Isolated signals and possible harmonics*

Many of the frequency spectra (33%, 146/443) of this sample contain isolated, individual signals that do not obviously belong to a group. These signals favor cooler stars, as 25% (56/222), 38% (30/80), and 46% (54/118) of early, mid, and late type stars, respectively, show these isolated signals. Again, this may be related to instrumental sensitivity, where a frequency group may exist, but only the strongest signal rises above the noise level (an effect expected to be more pronounced in later type stars with lower intrinsic amplitudes). The prototypical Be star, γ Cas, despite having a spectral type of B0.5 IVe and being intensively observed for well over 100 years, suffered from this observational bias where only isolated signals were identified (*e.g.* Smith et al. 2006; Borre et al. 2020) until being observed by TESS, which finally revealed the presence of groups (Labadie-Bartz et al., subm., Nazé et al. 2020). Nevertheless, it is clear that in many cases isolated signals rise well above the noise floor and are apparently unrelated to groups.

Harmonics of isolated signals appear in about 8% (34/443) of cases (or, in 23% of stars with isolated signals; 34/146), again being more common towards later spectral types (where 9% (5/56), 27% (8/30), and 30% (16/54) of early, mid, and late type stars with isolated signals have clear harmonics). These signals may reflect individual pulsation modes, or, at lower frequencies, may be related to rotation (either of the Be star, or perhaps a companion), a close bi-

nary (possibly in a hierarchical triple configuration with a relatively distant Be star), or are simply the strongest signal in an otherwise undetected group.

In our characterization scheme, isolated signals must be roughly constant in amplitude over the observing baseline of TESS. Otherwise, they would appear as two or more signals in the frequency spectrum (not necessarily of equal amplitude) as demonstrated in Section 3.4. It is, however, certainly possible that seemingly isolated signals can vary in strength over longer time baselines. The case of γ Cas exemplifies this, where an apparently isolated signal at 0.82 d^{-1} was known for many years, but with a decreasing amplitude to the point where it is no longer present in space photometry of the system (Borre et al. 2020; Henry & Smith 2012).

5.7. *No variability detected*

There are 9 systems where no variability is detected. Eight (one) of these systems are of late (mid) spectral type. This does not necessarily mean that these systems do not have variability, as signals below the detection threshold remain possible. Very low photometric amplitudes attributed to pulsation are often found in late type Be stars. For example, a few signals with amplitudes less than 0.05 mmag exist in Kepler data for the Be star ALS10705 (Rivinius et al. 2016), and the Be star CoRoT 102595654 has signals with amplitudes less than 0.2 mmag (Semaan et al. 2018).

5.8. *Non-classical Be Star Systems*

41 of the systems in our sample were identified as being something other than a classical Be star. An additional 35 systems have properties making their classical Be star classification uncertain, and of these 15 are rejected from the sample while the remaining 20 are included as there is insufficient evidence for rejecting their status as a classical Be star. Some of the types of systems that masquerade as Be stars in this sample include OB stars with strong magnetic fields or chemically peculiar stars, B[e] stars, interacting and/or close binaries, Herbig Ae/Be stars, supergiants, and OB stars embedded in nebulae. Sections A.1 and A.2 in the Appendix list and briefly discusses these systems. Some of these have been included in numerous works that aim to describe Be star populations (*e.g.* Frémat et al. 2005; Labadie-Bartz et al. 2017), underscoring the need to carefully vet samples of supposed classical Be stars against contamination from other types of systems.

6. DISCUSSION OF OVERALL RESULTS

Virtually all of the Be stars observed by TESS in sectors 1 – 13 are variable. Their photometric signals carry information about the underlying physical processes causing this variability, and a careful study of these observations elucidates the nature of Be stars as a population especially in regards to pulsation and mass ejection episodes. While there remains much to be explored with these data, the overview of Be star variability seen by TESS presented in this work provides a solid background of their photometric behavior as a population on short timescales and is a first step towards fully leveraging the unique dataset provided by TESS for these and similar objects. A discussion for each characteristic variability pattern is given in Section 5. The remainder of this section highlights correlations between different classes of variability.

6.1. *Correlations between variability classifications*

Figure 14 shows correlations between the observed characteristics of the sample (including spectral type). One of the most interesting correlations is between flickers and frequency groups. If there were no correlation, then 85% of the early-type stars with flickers are expected to also have frequency groups (55 out of 65), yet *every* star with flickers exhibits frequency groups (and, in 79% of systems with flickers there is an increase in the amplitude of groups coinciding with the flicker event). This is suggestive of a physical link between frequency groups and the short-duration mass-loss events that flickers are interpreted to represent.

This is not to say that frequency groups are necessary for a Be star to build up or sustain a disk. For example, HR 6819 (TIC 118842700) does not contain frequency groups, but rather is dominated by low frequency and stochastic variability and unambiguously supports a disk (Rivinius et al. 2020)[4]. A caveat is that, given the transient nature in many cases of Be star variability patterns, it remains possible that groups sometimes exist in HR 6819 outside of the short observing baseline provided by TESS. Similar examples include HD 84567 (TIC 11972111, Shokry et al. 2018), HD 53667 (TIC 177204351; see BeSS although it should be confirmed that this indeed is a classical Be star), HD 254647 (TIC 291385725, see BeSS), HD 44637 (TIC 438103655, see BeSS), and omi Pup (TIC 127493611, Koubský et al. 2012).

In stars with flickers that have the typical group configuration, there is a difference in the relative strength of $g1$ and $g2$ when compared with the full sample (as shown in Figure 7)[5]. In the 62 stars with flickers and typical groups, 7 have $g1$ stronger than $g2$ (11%), 35 (56%) have $g1$ and $g2$ being of similar strength, and 20 (32%) have $g2$ being stronger than $g1$. In other words, in stars with flickers there is a tendency for $g2$ to be relatively stronger compared to the group strengths of the full sample. Although not quantified at present, there is a qualitative trend of $g2$ seeing a more dra-

[4] HR 6819 is a multiple system that includes a narrow-lined B3 III star, which contributes about 50% of the total visible flux.

[5] The distribution of relative group strengths for just the early type stars is similar to that of the full sample.

matic enhancement than $g1$ during flicker events (*e.g.* Figures 4, 10), but this is not always the case (*e.g.* Figure 11).

In systems where stochastic variability is a prominent feature, there is a negative correlation with frequency groups, and a positive correlation with high frequency signals, as well as positive correlations with flickers and being dominated by low frequencies. These (anti-) correlations are apparent in the examples shown in Figure 13.

There is an anti-correlation between late-type stars and most aspects of the variability of the sample, but a positive correlation is found for very high frequency and isolated signals. This may be in part due to the lower intrinsic luminosity of later type stars, where signals from a hypothetical binary companion are more readily detected, as high and very high frequencies are not expected in late-type B stars.

7. CONCLUSIONS

Following in the footsteps of decades of observations from the ground, and in more recent years also from space, the TESS mission now, for the first time, provides high precision space photometry for the majority of known Galactic Be stars, allowing for a systematic study of their variability on timescales from minutes up to tens of days and down to amplitudes of approximately 100 parts-per-million. Analysis of TESS data for 443 classical Be stars observed in its first year of operation confirms that virtually all Be stars are variable (98% of this sample is variable at the level of precision available with TESS). The stars in this sample show a variety of characteristic signals, the rates of incidence of which are summarized in Table 1. Understanding the cause of these features and their incidence rates and patterns are important steps towards elucidating the physical processes in Be stars and other rapid rotators.

In general, Be stars show a higher level of pulsational variability than non-rapidly rotating stars of the same spectral type (Diago et al. 2009), and there is mounting evidence that rapid rotation enhances pulsational amplitudes and the number of excited frequencies (Neiner et al. 2012a, 2020; Rieutord 2009). It is becoming increasingly clear that pulsation is a common, and likely ubiquitous, element of Be stars (Rivinius et al. 2013; Semaan et al. 2018), which is supported by this study. In particular, the commonality of frequency groups may have important consequences in regards to the Be phenomenon, as this is the most common feature of the sample studied in this work. While it is possible that rotation contributes in some degree to the observed variability of the sample (via an inhomogeneous stellar surface and/or co-rotating clouds), rotation alone is insufficient to explain the majority of the observed signals. Rather, non-radial pulsation has properties that can explain much of the observed variability in this sample. NRP in rapid rotators naturally form frequency groups (Saio 2013; Saio et al. 2018a; Kurtz et al. 2015), NRP modes transport angular momentum to the surface layers which can assist in the triggering of outbursts (Bowman et al. 2019, 2020; Neiner et al. 2020), and NRP modes can couple in the resonant cavity in which they oscillate to produce combination frequencies with amplitudes higher than the sum of the parent modes (which can explain the lowest frequency group, $g0$ in many Be stars, and higher order groups Kurtz et al. 2015; Baade et al. 2018). It is clear that high frequency signals (taken to be $f > 6$ d^{-1}, but excluding harmonics of lower-frequecy signals) are related to pulsation, and not rotation (as such a rotational frequency would exceed the critical rotation rate). Further, stochastically-driven internal gravity waves (a type of non-periodic pulsation) have emerged as a plausible explanation for the low frequency excess and stochastic variability observed in many OB stars (Bowman et al. 2019, 2020).

Conversely, it is also important to study the Be stars which do not exhibit groups, but instead often are dominated by stochastic variability and/or one or more isolated signals. Understanding the physical properties of the stars belonging to these two categories (with and without groups), especially their rotation rate and evolutionary status, may lead to an improved understanding of how different Be stars eject mass. For example, a hypothesis that can be tested with spectroscopic or polarimetric time-series data is that systems with a high degree of stochastic variation, but without groups, may feed a disk in a more continuous fashion, compared to the episodic mass-loss episodes commonly seen in systems with well defined groups. Semaan et al. (2018) find that both of the Be stars that are evolved slightly past the main sequence, out of their sample of 15, show only stochastic variability, in contrast to the majority of the sample which exhibits frequency groups (12 out of the 13 main sequence stars). Constraining the evolutionary status of the systems observed by TESS may therefore be of great importance in interpreting the observed variability patterns

A not insignificant fraction of the Be stars in this sample (16% of the total, and 29% for early type stars) exhibit flickers, which we interpret as short-lived episodes of mass ejection (see Figure 9 for a proof of concept, and Figures 4, 10, 11 for additional examples). TESS is uniquely suited for capturing such events, which can last for only a few days and change the net brightness of the system by a few percent. Similar events have been observed from space in many Be stars prior to TESS (Semaan et al. 2018; Rivinius et al. 2013; Baade et al. 2016, 2017), but the large number of Be stars observed with TESS finally allows for a substantial sample to be studied. Future work will aim to better quantify the occurrence rate, shape, timing, amplitude, duty cycle, dependence on inclination angle, and dependence on the strength of any pre-existing disk of these events. Hydrodynamic and radiative transfer codes will allow us to model these events

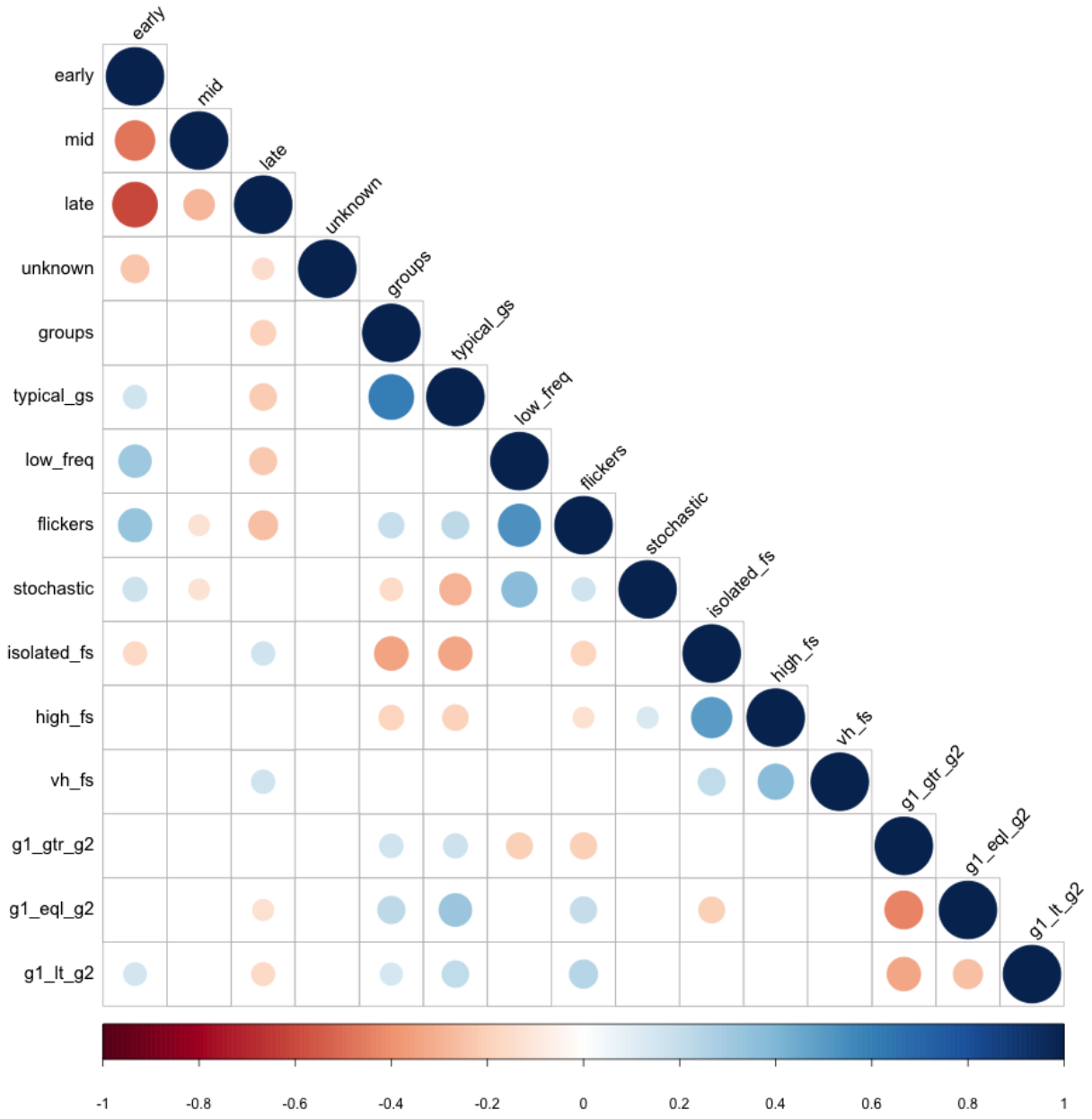

Figure 14. Correlations between various characteristics of the sample (blue = positive correlation). The size of each dot is proportional to the strength of the (anti-) correlation. From top to bottom, "early," "mid," "late," and "unknown" refer to the spectral type bins. "Groups" include stars with one or more frequency groups, and "typical gs" refer to those with the typical group configuration. "Low freq," "flickers," "stochastic," and "isolated fs" (isolated frequencies) refer to the variability classifications introduced in Section 4. "High fs" and "vh fs" refer to systems with high ($6 < f < 15$ d^{-1}) and very high ($f > 15$ d^{-1}) frequencies. The remaining categories describe the relative strength of $g1$ and $g2$ in systems with the typical group configuration, where $g1$ is stronger ("$g1$ gtr $g2$"), where both groups are of similar strength ("$g1$ eql $g2$"), and where $g1$ is weaker than $g2$ ("$g1$ lt $g2$").

and estimate the flux of mass and angular momentum from the star, which will provide estimates as to the degree which these relatively small-scale mass ejection events contribute to the total mass budget of the disk.

It is well known that mass loss episodes in Be stars can last for decades, years, months, weeks, or days (Rímulo et al. 2018; Labadie-Bartz et al. 2017, 2018). Whatever mechanisms are responsible for opening the mass-loss valve in

Be stars must be able to account for this large range in timescales. The increased amplitude of frequency groups coinciding with flicker/outburst events that is commonly seen in this sample (frequency group enhancement coinciding with flickers is seen in 76% of systems displaying these events) is suggestive of pulsation playing a key role, at least in the relatively short-lived events captured by TESS. However, we caution that in some situations the enhancement of frequency groups can instead be a consequence of mass ejection if the variability is in some part circumstellar (or perhaps a temporary increase in the amplitude of r modes). TESS, with its short observational baseline, is not sensitive to variability with timescales of tens of days and longer.

The contribution to massive star science with TESS has only just begun, yet is already producing important results for large samples (*e.g.* Bowman et al. 2020; Balona & Ozuyar 2020; Burssens et al. 2020; David-Uraz et al. 2019). Where other space photometry missions have paved the way towards studying Be stars at high photometric precision, TESS is continuing these opportunities for by far the largest sample yet of bright OB stars. The results presented in this paper are intended to be an overview of the types of variability that are seen in Be stars with TESS, and more in depth results regarding the nature of these signals and their significance will be explored further in forthcoming works by our group, and undoubtedly others. Especially exciting, given the brightness of TESS targets, is the relative ease of monitoring these stars with other observational techniques (spectroscopy, polarimetry, and multi-band photometry) from the ground which, when combined with TESS data, can greatly improve our understanding of these objects.

ACKNOWLEDGMENTS

*

J.L.-B. acknowledges support from FAPESP (grant 2017/23731-1). A.C.C. acknowledges support from CNPq (grant 311446/2019-1) and FAPESP (grant 2018/04055-8). The authors are grateful to the amateur spectroscopy community, whose observations have directly supported this and forthcoming works, in particular Stephane Charbonnel, Christian Buil, Paolo Berardi, Tim Lester, Alain Maetz, Robin Leadbeater, Erik Bryssinck, Olivier Garde, Franck Houpert, Olivier Thizy whose data was used in this publication. This work makes use of observations from the LCOGT network. This paper includes data collected by the TESS mission, which are publicly available from the Mikulski Archive for Space Telescopes (MAST). Funding for the TESS mission is provided by NASA's Science Mission directorate. This project makes use of data from the KELT survey, including support from The Ohio State University, Vanderbilt University, and Lehigh University, along with the KELT follow-up collaboration. This work has made use of data from the European Space Agency (ESA) mission *Gaia* (https://www.cosmos.esa.int/gaia), processed by the *Gaia* Data Processing and Analysis Consortium (DPAC https://www.cosmos.esa.int/web/gaia/dpac/consortium). Funding for the DPAC has been provided by national institutions, in particular the institutions participating in the *Gaia* Multilateral Agreement. This research has made use of NASA's Astrophysics Data System. This research has made use of the SIMBAD database, operated at CDS, Strasbourg, France. This work has made use of the BeSS database, operated at LESIA, Observatoire de Meudon, France: http://basebe.obspm.fr. This research made use of Lightkurve, a Python package for Kepler and TESS data analysis (Lightkurve Collaboration et al. 2018). This research made use of Astropy,[6] a community-developed core Python package for Astronomy (Astropy Collaboration et al. 2013, 2018). This work used BeSOS Catalogue, operated by the Instituto de Física y Astronomía, Universidad de Valparaíso, Chile : http://besos.ifa.uv.cl and funded by Fondecyt iniciación No 11130702, using the PUCHEROS instrument (Vanzi et al. 2012). The page is maintained thanks to FONDECYT No 11190945.

Facilities: TESS, Gaia, KELT

Software: astropy (Astropy Collaboration et al. 2013, 2018), Period04 (Lenz & Breger 2005), VARTOOLS (Hartman 2012)

[6] http://www.astropy.org

APPENDIX

Remarks are given below for individual systems.

A. NOTES ON INDIVIDUAL STARS

A.1. *Firmly mis-classified Be stars*

TIC 11286209 = sig Ori E: This is the prototype of the rapidly rotating early B stars with strong magnetic fields that confine the stellar wind, forcing it to co-rotate with the star, producing widely separated emission peaks (Landstreet & Borra 1978). It is heavily blended with the brighter star sig Ori, which is 2.7 mag brighter in the *V* band.

TIC 207176480 = HD 19818: High resolution spectroscopy acquired by our group shows this is an SB2, with an A0 main sequence star and a cooler giant in apparently synchronous rotation. Rotational modulation is apparent in TESS and KELT with the same period of 3.3 days. Hydrogen and other emission features are variable on short timescales and does not resemble a Keplerian disk. We suggest that, due to the rapid rotation of the cool giant star, a strong magnetic dynamo exists causing the observed rotational modulation (due to spots), and the highly energetic flares seen in the TESS data (Labadie-Bartz & Carciofi 2020). Chromospheric activity is likely the cause of the transient emission features (and the strong X-ray flux).

TIC 14709809 = RY Gem: A known "moderately interacting Algol-type eclipsing binary" (Plavec & Dobias 1987). TESS data likewise indicate this is an EB with a period of about 9 days, where the primary eclipse reaches a ~60% depth. Many BeSS spectra show Hα with a clear double-peaked profile and shell absorption, with variable V/R ratios, likely formed in an accretion disk around the A0V (present day) primary.

TIC 46022938 = IV Vir: A symbiotic binary (Mürset & Schmid 1999).

TIC 64333488 = AS 150: A long period symbiotic eclipsing binary with an evolved cooler star and accretion onto a hotter stellar component (Iijima 1985). The variability in TESS is mainly of low frequency and stochastic (as is typical for interacting binaries).

TIC 123545883 = V743 Mon: An unclassified B[e] star, or potentially a Herbig Ae/Be star (Varga et al. 2019), where severe stochastic variability is its main feature as in TESS.

TIC 187458882 = HD 57682: Many spectra in BeSS show the Hα emission is being single peaked, very variable in strength, narrow, and seemingly variable in position relative to the main Hα absorption. The MiMeS survey find this to be a strongly magnetic O9.5 IV star (Grunhut et al. 2017), and is therefore incompatible with a classical Be (or Oe) designation. Its only feature in TESS is strong stochastic variability. There is also a diffuse nebulae surrounding the star in the WISE red band, and a strong SED excess at the longest radio wavelengths.

TIC 200516204 = MWC 759 = HD 244524: Listed in the catalog of Herbig Ae/Be stars of Herbst & Shevchenko (1999) and classified as HAeB[e] from APOGEE spectra. In TESS data there is a single strong frequency at 2.19 d^{-1}, an exact harmonic of this signal (at 4.38 d^{-1}), and another signal near 4.55 d^{-1}.

TIC 231154751 = HR 2467: Classified as O5V((f))z+O9:V in the Galactic O-Star Spectroscopic Survey (GOSSS; Sota et al. 2014). Characterized in TESS largely by stochastic variability, but also has one strong signal at 0.65 d^{-1}, with the first sub-harmonic near 0.32 d^{-1}, which may indicate rotational modulation.

TIC 234813367 = AX Mon: Puss & Leedjärv (2002) classify this as an interacting binary system with a K giant and a B(e) star that is accreting matter, noting the P Cygni profile and unusual emission variations over the orbit. This system appears in numerous studies of populations of Be stars, but an interacting binary with an accretion disk around the hot component is incompatible with the decretion disks of classical Be stars. The TESS light curve is dominated by stochastic variation, but there are clear periodic signals, including one that stands out near 3.5 d^{-1}. Many BeSS spectra show a clear P Cygni profile in Hα.

TIC 234835218 = EM GGA 395:* A Herbig Ae/Be star (Li et al. 2002). Very clearly in a strong nebula, and the SED indicates a large amount of cool dust. Characterized as having strong stochastic variability and a single frequency near 2.6 d^{-1} in TESS.

TIC 238791674 = CD-49 3441: A Herbig Ae/Be star according to (The et al. 1994). High amplitude stochastic variability is the most prominent feature in TESS. A 6.77 day signal is found in the KELT data (Labadie-Bartz et al. 2017). Three low resolution BeSS spectra show strong Hα emission about 7 times the continuum level (which would be abnormally high for a B8 classical Be star).

TIC 246189955 = HD 328990: The SED is incompatible with that of a classical Be star, suggesting two stellar components (likely a cool giant, and a late B or early A main sequence star). There is only stochastic variability present, and the variability is dominated by low frequencies. The amplitude is very high (~10% max - min) relative to other confirmed classical Be stars of its spectral type, A0e.

TIC 253212775 = V495 Cen: An eclipsing interacting binary with a 33.5 day orbital period, a cool evolved star, and a hot mid-B dwarf with an accretion disk (Rosales Guzmán et al. 2018). The TESS light curve is dominated by the orbital modulation, but there are also clear (possibly aperiodic) oscillations with amplitudes of about 1% and frequencies between 0.5 – 3 d^{-1}.

TIC 253380837 = HD 113573: The TESS data unambiguously show this to be an EB with an orbital period of about 1 day, and primary and secondary eclipses that are slightly different in depth, but both around 3%. Although the field is somewhat crowded, the use of different sized apertures suggests the target star is the source of the EB signal. Besides the orbital period and its many harmonics, no other signals are present in the data.

TIC 276661825 = HD 290770: A known Herbig Ae/Be star (The et al. 1994).

TIC 305090822 = HD 157273:. Just one long sinusoidal signal exists, with P=15.72d (also very clear in KELT data). Clearly emission in Hα in the 3 low-resolution BeSS spectra. The SED appears to be formed from two components. This is probably an interacting binary with an accretion disk and possibly ellipsoidal variation.

TIC 320228013 = HD 308829: The TESS data show this to be a short-period EB (P_{orb} ~ 6.77 d) with significant asymmetric out-of-eclipse variability possibly caused by some combination of a reflection effect and rotation of an inhomogeneous stellar surface. This system is a cluster member (Cl* IC 2944 THA 51). The relatively dense region of the sky makes blending in TESS problematic, so it is not yet certain that the EB signal can be attributed to HD 308829. The SED has peculiarities. This is a known X-ray source (NRS2013), included in the ROSAT all-sky bright source catalog (Voges et al. 1999) and also observed with XMM-Newton, as discussed in Nazé et al. (2013).

TIC 380117288 = Al Cru: A very short period EB (P_{orb} ~ 1.4 d) with ~50% primary depth. Previously classified as a Mira Cet type variable (Samus' et al. 2017).

TIC 381641106 = CSI-62-12087: Listed as a WR star, MR 41 (Roberts 1962). The TESS light curve is purely stochastic at a high amplitude and low frequency.

TIC 408757239 = V716 Cen: Short-period ellipsoidal variable and EB, with P_{orb} ~ 1.5 d. A known EB on Simbad.

TIC 467065657 = HD 97253: Prominent stochastic variability with high amplitude. Classified as having a spectral type O5III(f) from GOSS survey (Sota et al. 2014), which is incompatible with being a classical Be star.

TIC 437994564 = MWC 137: Certainly an emission-line star with very high levels of emission, but not a classical Be star. Chojnowski et al. (2015) classify this as sgB[e], and it has previously been classified as a Herbig Ae/Be star (Herbst & Shevchenko 1999).

TIC 289877581 = d Lup: The TESS variability looks much more like rotation than pulsation. Given the 'p' in the spectral type (B3IVpe), this probably has surface spots (chemical or magnetic) leading to modulation at the 0.48 d^{-1} signal – the strongest

signal in the LC (assumed to be rotation). This star is included in catalogs of chemically peculiar stars (Romanyuk & Kudryavtsev 2008), supporting the plausibility of rotationally modulated brightness. The single BeSS spectrum is narrow lined in Hα, with no sign of emission. Arcos et al. (2018) analyze two epochs of spectra from 2013 and 2015, see no variability or emission in Hα, and fit blue photospheric absorption lines to arrive at a projected rotational velocity of $v\sin i$ = 30 km s^{-1} , which would be unusually slow for a rapidly rotating classical Be star.

TIC 333670665 = V863 Cen: A known magnetic He-strong star (Shultz et al. 2019). The TESS variability looks more like rotation or binarity than pulsation with a period of about 1.3 d, and a weak harmonic. 3 BeSS spectra show narrow lines with no sign of emission from 2012, 2017, and 2018.

TIC 394728064 = DR Cha: A clear EB with primary and secondary eclipses separated by about 20 days. No BeSS spectra exist. None of the six entries in the catalog of Skiff (2009) indicate emission. It is unclear what the reason for the historical Be star classification of this system, but perhaps its binary nature has lead to confusion.

TIC 443616529 = phi Leo: This system may have a debris disk, as there is some evidence for exocomets in the system (Eiroa et al. 2016). With a spectral type of A7IVne, this is too late to belong to the class of classical Be stars. The strongest signal by far is a single frequency at 6.48 d^{-1}, plus some lower level variability that may be stochastic or lots of lower frequency variation. Unclear why this is in lists of Be stars, although a debris disk may cause peculiarities (shell features) that can be confused with a gaseous decretion disk. No BeSS spectra from 2007 - 2020 show any sign of emission, nor do the three spectra on BeSOS. This is a high proper motion star.

TIC 455463415 = HD 135160: A very strange EB with a strong reflection effect, a primary eclipse depth of about 2-2.5%, and an orbital period of about 6 days. There are odd "bumps" in the LC not synchronized with the orbit, repeating roughly every 8 days. This is a known SB2, confirmed in (Wang et al. 2018). None of the references or spectral types in the 8 entries in the Skiff (2009) catalog include mention of emission, so the reason for this being included in the Jaschek & Egret (1982) catalog of Be stars is unclear.

TIC 53063082 = HZ CMa: Not a classical Be star. The TESS light curve looks much more like rotation or binarity P = 15 or 30 days. Strong single-peaked in a single high-resolution BeSS spectrum from 2009, with E/C 2.3, and asymmetric, being higher in the red. This system is included in many studies of Be stars (Touhami et al. 2011; Labadie-Bartz et al. 2017; Wang et al. 2018; Klement et al. 2019; Zhang et al. 2005; Sterken et al. 1996a). This is a binary with an accretion disk and ellipsoidal variability with P_{orb} = 28.6 d, and apparently has a Roche-lobe overfilling K giant companion (Sterken et al. 1994), where the authors interestingly note that the high $v\sin i$ value (300 km^s Meisel 1968) of the B star may be a consequence of accretion – *i.e.* this could be a Be star in the making (but currently has an accretion disk as it is being spun up). Listed as B6IVe+A in Slettebak (1982). Besides the orbital modulation, the TESS data contains only stochastic variability,

TIC 141973945 = bet Hya: The TESS light curve resembles rotation or binarity with a dominant signal at 0.43 d^{-1} (12.5 ppt), and lower-amplitude harmonics. 4 BeSS spectra all show a shell signature with weak emission. Simbad lists this as an alpha2 CVn type variable. A spectral type of kB8hB8HeA0VSi is given in Garrison & Gray (1994), and is therefore not a classical Be star.

TIC 151300497 = V1075 Sco: Stochastic variability is prominent in TESS, as are low frequency signals. There are narrow ill-defined groups that stand out above the noise. Not a classical Be star, despite Hα emission in BeSS spectra. The GOSS survey gives a spectral type of O7.5V((f))z(e) (Sota et al. 2014).

TIC 220322383 = 15 Mon: B1Ve. Very low amplitude signals in TESS, the strongest of which is 0.5 ppt at 12.5 d^{-1} (with a nearby signal at 11.9 d^{-1}). This is a known X-ray source and spectroscopic binary (O7V+B1.5/2V, Skiff 2013), is embedded in a nebula, and is a cluster member. Also classified as an O7V((f))z variable (Sota et al. 2014).

TIC 224244458 = bet Scl: The TESS data more closely resembles rotational modulation with a period of about 2 d. Spectral type of B9.5IIIpHgMnSi (Abt & Morrell 1995). Rejecting as a Be star – this is a chemically peculiar star exhibiting rotational

modulation.

TIC 90296023 = FY Vel: KELT data show this to be a 33.75 d period EB ellipsoidal variable, as reported in (Labadie-Bartz et al. 2017), and is a known Beta Lyrae type EB (Thackeray et al. 1970). Not a classical Be star. Presumably there is mass transfer via Roche-lobe overflow, leading to the strong Hα emission seen in the 4 available BeSS spectra, which show Hα E/C ~8 – 10.

A.2. *Suspected mis-classified Be stars*

TIC 11411724 = StHA 52: Embedded in a strong reflection nebula, NGC 2023. Unusual frequency spectrum. Four frequencies of similar strength spread out over 0.5 d^{-1}, centered at 8.75 d^{-1}, and other high frequencies between 10 – 11.5 d^{-1}. Not in BeSS, and no emission features in APOGEE. Given the strength and size of the reflection nebula in the visible, it is unclear exactly what is contributing to the TESS photometry. This is not included as a Be star.

TIC 140132301 = HD 72126: Extremely strong, stable, single frequency at 3.04 d^{-1}, with a semi-amplitude of about 10%. Very unusual LC and frequency spectrum for a Be star. No other Be stars in the sample have such a simple frequency spectrum with only one extremely strong frequency. B2nne from 1978 MSS, but B5 from 1993 (Cannon & Pickering 1993). There is some diffuse nebula in the vicinity, so perhaps this is mis-classified as a Be star. No BeSS spectra. SED does not appear to show any fluctuation in the IR/radio. In the Be star catalog of Jaschek & Egret (1982), but is not included as a Be star here.

TIC 147244857 = HD 70234: Unusual LC for a Be star. Has only two isolated frequencies with constant power at 1.55 and 2.27 /cd causing a beating pattern with a very short envelope. First reported as an emission line star in Henize (1976), where it is listed as B9III(e). One low resolution BeSS spectrum clearly shows Hα in emission at E/C=2.5. We cannot rule out the possibility that this is a classical Be star.

TIC 151131426 = HV Lup: There is one dominant signal with a double-wave pattern at P = 5.66 days with a ~10% semi-amplitude, plus stochastic variability. It is possible that this is an interacting binary with a 5.66 day orbital period. The behavior of the light curve and frequency spectrum most closely resembles other interacting binaries rather than a classical Be star. No BeSS spectra are available. Not included in statistics.

TIC 155573117 = CD-27 5181: This looks more like an EB or a sig Ori E type case, with two single strong signals at exact harmonics (0.6 and 1.2 d^{-1}), which resemble eclipses of about 1%, plus stochastic variability. No BeSS spectra are available. Included in the Be star catalog of Jaschek & Egret (1982), and is apparently of a relatively early spectral type, being classified as OB+e in Stephenson & Sanduleak (1971). The same photometric frequency is reported in (Labadie-Bartz et al. 2017). Without a spectrum, we cannot determine whether or not this is a classical Be star, and is thus included in the statistics.

TIC 191312952 = HD 129772: One dominant signal at 3.15 d^{-1}. Unclear if it is an unresolved narrow group, or a single frequency modulated in amplitude (clearly seen in the LC, but could be beating). There are multiple harmonics of this signal/group. Strange system. In the Renson & Manfroid (2009) catalog of Ap, HgMn, and AM stars, where it is listed as having a spectral type of B8 Ca, suggesting an abundance of calcium, but its classification is also of "doubtful nature". No BeSS spectra are available. Insufficient evidence to rule this out as a classical Be star.

TIC 215983126 = HD 144970: The star is very reddened, but is apparently B0V or B0Ve (Cannon & Pickering 1993; Feast et al. 1961). No BeSS spectra available. TESS data show only stochastic variability and possible short duration flares. Could be some other type of object, but this is inconclusive and so is included as a Be star in this work.

TIC 216158265 = HD 155436: There is only β Cephei type pulsation, with nothing short of 6 d^{-1}, but many signals are present between 6.5 – 11 d^{-1}. In the Jaschek & Egret (1982) catalog of Be stars, and listed as having a spectral type of B0.5IIIn(e) in Garrison et al. (1977). One low resolution BeSS spectrum shows Hα in emission with E/C~1.8. While the TESS frequency spectrum is unusual in not having any power at low frequencies, we cannot claim this is not a classical Be star and it is included in this sample.

TIC 216875138 = HD 156172: A known β Cephei pulsator (Pigulski & Pojmański 2008), confirmed by the TESS data which show a pair of signals near 7 d^{-1}, with a clear harmonic of the stronger of the two. There may be weak frequency groups in the

TESS data, near 1 and 2 d^{-1}. Perhaps this is a binary, similar to β Cephei itself, where the primary is a high frequency p mode pulsator and the secondary is a later type Be star with a decretion disk. Included in the statistics in this work.

TIC 256994805 = V715 Mon = HD 49567 = HR 2517: Only a weak disk is present in one professional BeSS spectrum. This system is apparently is a high mass X-ray binary (Khalak et al. 1998) and has also has been observed to show "flares" (Sterken et al. 1996b), which are strange since they are brighter in the bluer bands (Be outburts are larger in redder bands). This also does seem to be an evolved star. Included in the statistics in this work.

TIC 282808223 = HD 50820 = HR 2577: A binary B3IVe+K2II system with a period of 58 years where the balmer emission lines of the B star are variable in a fashion unrelated to the orbit (Hendry 1982). The TESS LC shows mostly slow, gradual, low-amplitude variation plus mild stochastic variation. Included as a Be star in this work, although it is possible variability from the K giant contributes to the TESS data.

TIC 284230347 = HD 55806: Very high amplitude low-frequency variation, 3% semi-amplitude, plus stochastic variation. A CoRoT Be star. In Frémat et al. (2006), they note for HD 55806 that they could not find any set of fundamental parameters allowing a simultaneous fit of the observed He and Mg spectral lines. All of the He lines show unusual line shapes, probably related to the presence of a close companion. It is the only star in their sample of 64 to show this behavior. The low-frequency signal is also very apparent in the KELT data, being single-waved at 6.996 d or maybe double-waved at 13.98 d. This suggests a close binary, and perhaps an accretion disk scenario. The TESS data seem more similar to other interacting binaries compared to "normal" classical Be stars. This is not included as a classical Be star in this work.

TIC 308951795 = HD 306145: Unusual LC, with many short, small 'bumps' that are not obviously related to pulsation or flickers. There are also definitely high and maybe very high frequencies, and stochastic variation out to high frequencies. No emission in the single low-resolution BeSS spectrum. Very close visual double (clearly seen in 2MASS). The strongest signal is at 0.25 d^{-1}, or P=3.9 days (also apparent in KELT). The variability in TESS is very unusual, but cannot be ruled out as a classical Be star based on existing data.

TIC 315679257 = HD 146596: Just low frequency signals (1%) and stochastic variability. No BESS spectra. Has Hα emission from HARPS according to Rainer et al. (2016), and is therefore classified as a Be star, but without estimates of stellar parameters. The SED shows an excess in the mid-IR with a clear down-turn. This looks suspicious for a classical Be star, but without seeing a spectrum it is hard to determine. The Hα line (from http://sisma.brera.inaf.it/index.jsp) looks typical for a Be star, with E/C 2.3, and V/R 1. Possibly some weak and very narrow emission in other non-Balmer lines (near 4922 Å, 5020 Å, and some others), which appear to have P Cygni profiles, like near 4922 Å, 5020 Å. Suspected non-Be, but cannot at present be ruled out.

TIC 316792722 HD 99771:. good quality 2- and 30-min data. Claiming that the two lowest frequency groups are in the typical configuration, at 0.61 and 1.23 d^{-1}. There is a third group near 2.19 d^{-1}, and then many isolated frequencies with exact harmonics. Possibly the signal near 4.96 d^{-1} is rotationally split? Slightly unusual SED excess at long wavelengths? It is embedded in a large cloud. Included in the Jaschek 1982 catalog, but there don't seem to be any more recent works or spectra that are relevant. No signals in KELT, as expected.

TIC 319854805 –¿ HD 47359: Suspicious and interesting case with extremely simple flickers with precurser phases and no apparent change in the frequency spectrum, and a pair of high frequency signals at 11.8 and 13.3 d^{-1}. Just one dominant frequency and a very low amplitude harmonic of it, plus obvious low-frequency signals. 3 BeSS spectra show weak Halpha, sometimes double-peaked, sometimes single, with E/C 1.2. Both the 12 d 'flicker' signal and the f = 1.545 d^{-1} are very clear in KELT. The P=12.13d signal is interesting with how regular it is in KELT and how much it resembles the TESS signal. This probably isn't a normal Be star flicker. Listed as B0.5Vp in Polarization and rotational velocities of Be stars (Yudin, 2001). With Vsini = 443 ± 40 km/s (Fremat 2006), this would have to be very close to edge-on, yet the Halpha profile is clearly not that of a shell star. The nature of this object is unclear, and it is not included in the statistics of this sample.

TIC 322104948 = HD 306989 = V644 Cen:. Suspicious LC. Clear 25 d period in KELT, and also apparent in TESS, but also with stochastic variability. Many high frequency signals in TESS are evident. No BeSS spectra. SED is suspicious, sort of looking like two components. YSO candidate from SVM selec-

tion of WISE YSO Candidates (Marton+, 2016) . Possibly a very long period (200 years) eclipsing binary with an eclipse duration of 17+ years according to https://ui.adsabs.harvard.edu/abs/1951MNRAS.111..111O/abstract and https://ui.adsabs.harvard.edu/abs/1987IBVS.3006....1D/abstract. Likely not a classical Be star- not included in Be star statistics.

TIC 322233181 = HD 306962: Another tricky case that looks oddly similar to the above (TIC 322104948) , despite having different LC and freq. spectrum behavior. Dominated by stochastic variability, and a single signal at 5.97 d^{-1}. Also in SVM selection of WISE YSO Candidates (Marton+, 2016) . Not enough evidence to discount this being a classical Be star, but it is suspect. Mostly stochastic variability but some clear periods as well.

TIC 381747495 = HD 105753: Odd LC. Lots of low frequency stochastic variation, and a somewhat strong group near 8.5 d^{-1}. Clear LTV in KELT. There is no information to rule this out as a classical Be star, but the light curve and frequency spectrum are suspicious. No similar cases are seen in the sample. No BeSS spectra.

TIC 342257745 = HD 322422: Unusual LC with a single low-freq signal dominating (f = 0.39 d^{-1}), probably a weak group at 1.61 d^{-1}, and some high frequency signals at 6.91, 8.3, and 13.4 d^{-1}. The low-freq signal is not in KELT. Embedded in a nebula. Listed as having emission in 7 references in Skiff (2009). Vsini = 170 ± 11 in Zorec+2016. Possibly a Herbig Ae/Be star- listed in the Extreme emission line objects (EELOs) table in Member of Herbig Ae/Be stellar group (The+ 1994). Has 'near IR excess - WiH', but I don't know what WiH means. The extreme emission line objects are usually most likely LBVs, B[e] stars, HAEBEs, PNs, or Symbiotics (from Pg. 322 of The et al. 1994). Classified here as unlikely to be a classical Be star and not considered in the statistics.

TIC 451280762 = HD 99146:. Strange. Near-spherical nebulosity nearby, but obviously not centered on the target star. No BESS spectra. Clear LTV and possibly outbursts in KELT. Need a spectrum to determine whether or not this is a classical Be star.

TIC 455809360 = CD-61 4751: Suspicious LC dominated by slow stochastic variation. SED looks like 2 components. Probably an interacting binary? Unclear what the nature of this system is. Not included in statistics.

TIC 457546452 = HD 126986: Low frequency periodic double-waved LC- almost definitely binary or rotation related. Unlikely to be a classical Be star just based on TESS data. No BESS spectra. SED seems to have 2 components. Assume this is not a classical Be star.

TIC 466715331 = HD 308217: Look up online, unclear if classical Be. strange LC. BESS spectrum in absorption. S.T. = B3. Lots of stochastic variation, dominated by low frequencies, but there is a frequency 'group' near 6.2 c/d which looks like p-modes, and also a signal at 8.44 d^{-1}. There are events that sort of resemble flickers, but could be related to rotation or something, with a quasi-period of about 10 days. I think the proper motion is kind of high, pmra = -6.192, pmdec = +2.180. Can't get the SED to load...

TIC 468095832 = 2E 1118.7-6138 = WRAY 15-793: HMXRB and I think gamma-ray source.. O9.5III/Ve C 1981A&A....99..274J. BK-943. Clear periodicity in KELT, but kinda odd. Looks like 'flickers', but very symmetric, amplitudes of 2 mag (!!) and durations of 100 d. Period is 200 d. Unclear at the moment if this is a Be + XRB or an OB + XRB with stellar winds or something. X-ray pulsar and transient x-ray source by Liu et al 2006. I guess assume this is a classical Be star for now.

TIC 213153401 —¿¿ Looks a LOT like sigma ori e. HD 154538: 2 BeSS spectra are too low-res to say much, but they are both clearly in absorption. Could be an old-fashioned EB, but without any ellipsoidal variation and a very short period of f = 2 d^{-1} and equal primary/secondary depths (or no secondary at all). Very close visual double, so hard to say where the signals are coming from exactly. Wonder what the deal with this system is. Possible that the fainter of the pair is the one with emission: see Skiff (2009). Classify as possibly not a classical Be star and do not include in statistics.

TIC 427400331 –¿ HD 290662:. Has a very high-freq group at 75 d^{-1} with 0.6 ppt amplitude, plus regular low-freq groups with amplitudes of around 0.25 - 1.5 ppt. Seems to be in the Renson catalog of Ap and Am stars. That could explain the super

high freq group if its an roAp star. (Renson+ 2009) gives B9 Fe ST. 1 low-res BeSS spectrum doesn't obviously show any emission. Skiff (2009) also notes an A0Vp designation from 1971 saying Fe II lines prominent. Unclear what the nature of this star is without being able to see a spectrum. Assume it is a Be star, but there is good evidence for a roAp star being one star in the system, but who knows whether or not there is a genuine classical Be star as well. There could be some stochastic variability, one rotation frequency near 0.2 d^{-1}, and two typical g-mode groups centered at 2.12 and 1.05 d^{-1}.

TIC 269087549 = 19 Mon: Possibly a hybrid SPB/BCEP pulsator, with a pair of BCEP looking pulsations centered around 5 c/d, with a combination frequency near 10 c/d. Known BCEP star in Simbad. H and He line profiles on BeSS look like either significant LPV from NRP, and/or binary-induced variations. No sign of any emission from 2003 - 2020 in hundreds of spectra. In the Jaschek 1982 catalog of Be stars. In Skiff (2009) catalog, there are 11 entries, and only one of them hints at emission, with the note "em?" from 1975ApJ...196..773I. Found to be an SB2 based on 9 spectra **(Chini+, 2012)**. Assuming this is not a classical Be star, and the the potential "em?" classification from 1975 was the result of being an SB2. Not included in any statistics.

TIC 307225534 = V767 Cen: Suspicious. 15% amplitude variability with timescale of maybe 30 days, plus some much lower amplitude frequency groups at around 0.8, 1.7, 3.5, and 5.2 c/d. X-ray source. Absorption lines seem narrow in BeSS, and Halpha emission is single-peaked and about E/C 2.5 usually, but up to 4. B2IIIep from **Slettebak 1982,** Vsini=70 km/s from **Fremat 2005**. Unclear how to proceed with this. The brightness drops by 15% in about 10 days, which is a bit unusual. If this is a classical Be star, and there is no convincing evidence that it is not, then it is at a very low inclination angle due to having a low vsini, single peaked emission, and narrow absorption lines. **Investigate the X-ray flux to check its properties.** It is included in statistics.

TIC 376077639 = V862 Ara: B7IIIe. Extremely clear case of sum and difference frequencies and harmonics of the main group. No emission in the 2 BeSS spectra with high enough resolution. B7II/III in simbad, but also listed as a Be star. However, the Be designation does not seem to have much evidence. The only reference for being an emission line star at all is from Hipparcos photometry, where it earned the VSX designation "BE:", where the colon indicates uncertainty. I think there is not reasonable evidence to claim this is a Be star. Not including in statistics. In General Catalogue of Variable Stars (Samus+, 2007-2017) as BE:. I think there is not reasonable evidence to claim this is a Be star. Not including in statistics. Spent way too long looking, and could find no evidence that this has been observed to be in emission at any point.

TIC 405520863 = 39 Cru: Looks more like rotation or binarity. Only a single signal at 1.30 c/d, and a few weak harmonics. 2 BeSS spectra have Halpha emission with E/C 3.5, and a symmetric doulble peak (2017). 2 spectra on BeSOS from 2014, 2015 have the same profile. Unusual in its simplicity and constant Halpha emission. There is no obvious evidence against this being a classical Be star, but its TESS light curve is remarkably simple. Assuming this is a Be star, and is included in statistics.

23091719 - NW Pup. B2IVne.lower frequency variability, including stochastic features, dominates. No obvious groups. Kind of unusual, the lack of groups despite the clear varibility. No sign of emission, and narrow-lined, including a narrow He 6678 line in one high-res spectrum from 2020-04-15. Unclear if this is truely a classical Be star given the narrow lines and lack of emission in 2019-2020. No sign of emission in 2014 in two epochs of BeSOS spectra, and their best-fit model gives Vsini = 50 km/s. Far-radio excess in the SED. Included in the catalog of Egret et al. 1981 where it is listed as a He-abnormal chemically peculiar star, and in the Renson+2009 catalog of Ap and Am stars, being listed as B3 He var. BeSS ST and emission-line designation seems to come from only 1969ApJ...157..313H. Very narrow-lined in the blue in Chauville+, 2001. Suspected non-Be star. Not included in statistics.

26175330 - 17 Sex. A1Ve. No signals in TESS. Extremely deep and narrow Halpha, dropping to about 0.175 times the continuum level. No sign of any emission in many BeSS spectra, including a professional spectrum from ELODIE. Listed as a Herbig Ae/Be star on Simbad, and classifed as an A-shell star in (2009AA...495..901M). LIkely falsely classified as a Be star because of shell features in this A-type star. Suspected non-Be star. Not included in staistics.

140031673 - HD 71510. B2Ve. There appear to be groups but their pattern and delineation is unclear. None of the spectra in BeSOS (2014, 2015) or BeSS (2014/15/17/19) show Halpha in emission. Vsini = 150 km/s from BeSOS. In Jasheck 1982 catalog of Be stars. Apparently a known visual binary (e.g. Wackerling 1970). None of the 6 references in Skiff 2009 list emission. The visual binary pair is listed as B3V + G3V (1992AA...261..245P), but that does not exclude the B-type star being a Be star. There is an IR nebulae centered on the target (Bodensteiner+, 2018). This star is of unclear nature. Perhaps the IR excess from the

surrounding nebula is the reason for its Be desgignation, but without further evidence this cannot be excluded as a classical Be star. This is included in the statistics for the sample. Variability in TESS is largely stochastic, but there do seem to be coherent signals in the traditional g mode regime.

466715331 = HD 308217. Look up online, unclear if classical Be. strange LC. BESS spectrum in absorption. S.T. = B3. Lots of stochastic variation, dominated by low frequencies, but there is a frequency 'group' near 6.2 c/d which looks like p-modes, and also a signal at 8.44 d^{-1}. There are events that sort of resemble flickers, but could be related to rotation or something, with a quasi-period of about 10 days. I think the proper motion is kind of high, pm-ra = -6.192, pm-dec = +2.180. A known visual double (delta-mag = 2.0). The only reference to emission is from 1970AJ.....75..703G, noting that there is emission in Hbeta. I suspect this is not a classical Be star, but there is insufficient evidence to determine the nature of this object.

440399815 = HD 113605. Low level stochastic variability is the main signal. In KELT there is a fairly strong periodic signal at P=32.087 days, which could be related to binarity. Without any spectra, the nature of this object is unclear, but there is no convincing evidence against this being a classical Be star.

A.3. *Stars with no detected signals*

Continue to populate this list.

TIC 207580161 = HD 119835: No signals detected in TESS (Tmag = 9.42), although there are some instrumental effects (most likely spacecraft momentum dumps which occur roughly every 3 days). 2-minute cadence data is not available. Originally classified as an emission line star in Henize (1976). No BeSS spectra are available, but there is no evidence in the literatuer against this being a classical Be star. Classified as having a spectral type B8/9II/IIIn:(e?), and the Hβ line is partially filled **citation! ??**.

TIC 247589847 - BD+13 976: The APOGEE Br11 emission is normal looking, double-peaked, and slightly variable over the 393 days of observation (ABE-083 **citation**) in this A0 star (Tmag = 10.28). No signals are detectable in the TESS (2- or 30-minute) data, which are of high quality and largely free from systematic effects.

285187855 - HD 138477. There are no apparent signals in TESS except for systematic effects likely from scattered light in this B7IIIe star with Tmag = 8.12, which does not have a 2-minute light curve.

A.4. *Be star systems of interest*

Continue to populate this list.

65803653 - 27 CMa. Looks like a composite spectrum with a single signal at 0.76 d^{-1} and its first harmonic, plus two groups at 1.33 and 2.69 d^{-1}. There are also isolated signals around 10.9 and 13.5 d^{-1}, plus a pair of signals near 5.16 and 5.90 d^{-1}. Shell star with strongly varying disk, including strong asymmetries from 7 BeSS spectra between 2006 - 2019. Good candidate for binarity. Known BCEP pulsator (2005ApJS..158..193S). Balona et al 1994 (1994IBVS.4022....1B) find the same BCEP-like frequency - they report 10.893 c/d, and a low frequency signal of 0.796 d^{-1}.

118842700 - QV Tel. B3IIIpe. One strong low frequency signal (maybe around 0.1 c/d), and strong stochastic varibility. No obvious patterns in the LC. BeSOS Halpha is symmetric and double-peaked with E/C 1.5. There are two narrow lines to the right of Halpha- C or Ca lines? I forget exactly what species those are. Narrow lined in He though- they estimate Vsini = 50 km/s, which even seems too high. I'd expect a classical Be star with such an Halpha profile to certainly have a higher vsini. Halpha is definitely variable in the 17 BeSS spectra from 2011 - 2020. Oh, this is HR 6819, the potential triple (BH + B) + Be system. That can explain the narrow lines since the giant B star contributes about 50% of the flux. Should I include this in the statistics? Yes.

127493611 - omi Pup. BIVnne. Strong, clear, coherent sinusoidal signal at f = 0.495 c/d or so (amplitude ~6 ppt), and a few high frequency signals near 8.5, 10.2, and 14.5 d^{-1} (amplitudes beteween 0.1 and 0.3 ppt). Halpha is almost flat-topped, but slanted down to the blue. Does not change much over 2 years in BeSOS spectra. Likely a Be + sdO binary (2012AA...545A.121K) with a 28.9 d period. The 2 d periodic signal in TESS is kind of odd. He emission can change very rapidly, with clear variability seen from night to night in some BeSS spectra. No sdO spectrum detected in Wang + 2018. Despite having no frequency groups, this system seems to be able to support a rather strong disk at all observed times.

139385056 - FY CMa, B0.5 IVe. Famous Be+sdO binary. Actually a highly unusual LC. There is low frequency stochastic variability. The most prominent feature is a pair of signals centered at 8.50 and 8.99 d^{-1}, of equal strength of about 2.2 ppt. There are many frequencies between 3 – 9 d^{-1}, which may form some doublets or triplets.

281047621 - ome Ori. Variable disk, double-peaked and usually roughly symmetric. Sometimes He wing emission. Unusually simple LC, with a very strong peak at 1.07 c/d, and a harmonic at 2.14 c/d. Small frequency groups at around 0.5 and 1.54 c/d. Looks like it is ionizing some nearby gas. Hard to say if there are groups or just single frequencies. Assuming they are groups, since the amplitude clearly, but slowly and mildly, varies for the main 1.07 c/d signal. Saying groups yes, but canonical groups = 0.5. **Perhaps hosts a weak magnetic field** (2012MNRAS.426.2738N). Interestingly, the rotation frequency derived in (2003A

401635731 –¿ Extremely unusual and interesting flicker-looking events that are decidely non-sinusoidal (and have an exact harmonic). V1012 Cen. BK-775. Single low-res BeSS spectrum shows Halpha in emission at 3xContinuum. Strong 5.49d signal in KELT, which is also the dominant signa in TESS. Actually this signal also seems to have a beat envelope, in both KELT + TESS. Also a signal at 2.33 d^{-1}, which is strongest when the beat envelope of the low-freq signals are low, but is present throughout, and does seem relatively strong near peak brightness.

439164152 - CPD-63 2495. has one eclipse near the end of the dataset, reaching a depth of about 0.5%. No visible BeSS spectra, 3 IUE. High Mass X-ray Binary according to Simbad (2013MNRAS.431..327L). The eclipse is now rather interesting. O9.5Ve (2014MNRAS.439..432C) in an interesting study of the object from its 2010-2011 periastron passage. Known to have an orbit of Porb = 1236.9 d, e = 0.87 (Johnston et al. 1992, 1994). Seems like a real classical Be star, and not a supergiant. Interesting system. Probably the eclipse is unrelated to the HMXRB and may be a blend or some other source. With an orbital period of about 3.4 years, an eclipse is extremely unlikely.

REFERENCES

Abt, H. A., & Morrell, N. I. 1995, ApJS, 99, 135, doi: 10.1086/192182

Aerts, C., Bowman, D. M., Símon-Díaz, S., et al. 2018, MNRAS, 476, 1234, doi: 10.1093/mnras/sty308

Arcos, C., Kanaan, S., Chávez, J., et al. 2018, MNRAS, 474, 5287, doi: 10.1093/mnras/stx3075

Astropy Collaboration, Robitaille, T. P., Tollerud, E. J., et al. 2013, A&A, 558, A33, doi: 10.1051/0004-6361/201322068

Astropy Collaboration, Price-Whelan, A. M., Sipőcz, B. M., et al. 2018, AJ, 156, 123, doi: 10.3847/1538-3881/aabc4f

Baade, D., & Rivinius, T. 2020, in Proceedings of the conference Stars and their Variability Observed from Space, ed. C. Neiner, W. W. Weiss, D. Baade, R. E. Griffin, C. C. Lovekin, & A. F. J. Moffat, 35–38

Baade, D., Rivinius, T., Pigulski, A., et al. 2016, A&A, 588, A56, doi: 10.1051/0004-6361/201528026

Baade, D., Rivinius, T., Pigulski, A., et al. 2017, in Second BRITE-Constellation Science Conference: Small Satellites - Big Science, Vol. 5, 196–205. https://arxiv.org/abs/1611.01113

Baade, D., Pigulski, A., Rivinius, T., et al. 2018, A&A, 610, A70, doi: 10.1051/0004-6361/201731187

Baglin, A., Auvergne, M., Boisnard, L., et al. 2006, in 36th COSPAR Scientific Assembly, Vol. 36, 3749

Balona, L. A., & Ozuyar, D. 2020, MNRAS, 493, 2528, doi: 10.1093/mnras/staa389

Bernhard, K., Otero, S., Hümmerich, S., et al. 2018, MNRAS, 479, 2909, doi: 10.1093/mnras/sty1320

Bjorkman, K. S., Miroshnichenko, A. S., McDavid, D., & Pogrosheva, T. M. 2002, ApJ, 573, 812, doi: 10.1086/340751

Bodensteiner, J., Shenar, T., & Sana, H. 2020, arXiv e-prints, arXiv:2006.13229. https://arxiv.org/abs/2006.13229

Borre, C. C., Baade, D., Pigulski, A., et al. 2020, A&A, 635, A140, doi: 10.1051/0004-6361/201937062

Borucki, W. J., Koch, D., Basri, G., et al. 2010, Science, 327, 977, doi: 10.1126/science.1185402

Bowman, D. M. 2020, arXiv e-prints, arXiv:2008.11162. https://arxiv.org/abs/2008.11162

Bowman, D. M., Burssens, S., Simón-Díaz, S., et al. 2020, arXiv e-prints, arXiv:2006.03012. https://arxiv.org/abs/2006.03012

Bowman, D. M., Aerts, C., Johnston, C., et al. 2019, A&A, 621, A135, doi: 10.1051/0004-6361/201833662

Bozic, H., Harmanec, P., Horn, J., et al. 1995, A&A, 304, 235

Brasseur, C. E., Phillip, C., Fleming, S. W., Mullally, S. E., & White, R. L. 2019, Astrocut: Tools for creating cutouts of TESS images. http://ascl.net/1905.007

Breger, M. 2000, Astronomical Society of the Pacific Conference Series, Vol. 210, δ Scuti stars (Review), ed. M. Breger & M. Montgomery, 3

Burssens, S., Simón-Díaz, S., Bowman, D. M., et al. 2020, A&A, 639, A81, doi: 10.1051/0004-6361/202037700

Cameron, C., Saio, H., Kuschnig, R., et al. 2008, ApJ, 685, 489, doi: 10.1086/590369

Cannon, A. J., & Pickering, E. C. 1993, VizieR Online Data Catalog, III/135A

Cantiello, M., & Braithwaite, J. 2011, A&A, 534, A140, doi: 10.1051/0004-6361/201117512

—. 2019, ApJ, 883, 106, doi: 10.3847/1538-4357/ab3924

Cantiello, M., Braithwaite, J., Brandenburg, A., et al. 2011, in IAU Symposium, Vol. 272, Active OB Stars: Structure, Evolution, Mass Loss, and Critical Limits, ed. C. Neiner, G. Wade, G. Meynet, & G. Peters, 32–37, doi: 10.1017/S174392131100994X

Cantiello, M., Langer, N., Brott, I., et al. 2009, A&A, 499, 279, doi: 10.1051/0004-6361/200911643

Carciofi, A. C. 2011, in IAU Symposium, Vol. 272, Active OB Stars: Structure, Evolution, Mass Loss, and Critical Limits, ed. C. Neiner, G. Wade, G. Meynet, & G. Peters, 325–336, doi: 10.1017/S1743921311010738

Casares, J., Negueruela, I., Ribó, M., et al. 2014, Nature, 505, 378, doi: 10.1038/nature12916

Chojnowski, S. D., Whelan, D. G., Wisniewski, J. P., et al. 2015, AJ, 149, 7, doi: 10.1088/0004-6256/149/1/7

Chojnowski, S. D., Labadie-Bartz, J., Rivinius, T., et al. 2018, ApJ, 865, 76, doi: 10.3847/1538-4357/aad964

Cyr, I. H., Jones, C. E., Carciofi, A. C., et al. 2020, MNRAS, 497, 3525, doi: 10.1093/mnras/staa2176

David-Uraz, A., Neiner, C., Sikora, J., et al. 2019, MNRAS, 487, 304, doi: 10.1093/mnras/stz1181

De Cat, P. 2002, in Astronomical Society of the Pacific Conference Series, Vol. 259, IAU Colloq. 185: Radial and Nonradial Pulsationsn as Probes of Stellar Physics, ed. C. Aerts, T. R. Bedding, & J. Christensen-Dalsgaard, 196

de Mink, S. E., Langer, N., Izzard, R. G., Sana, H., & de Koter, A. 2013, ApJ, 764, 166, doi: 10.1088/0004-637X/764/2/166

Diago, P. D., Gutiérrez-Soto, J., Fabregat, J., & Martayan, C. 2009, Communications in Asteroseismology, 158, 184. https://arxiv.org/abs/0902.4354

Dziembowski, W. A., Moskalik, P., & Pamyatnykh, A. A. 1993, MNRAS, 265, 588, doi: 10.1093/mnras/265.3.588

Edelmann, P. V. F., Ratnasingam, R. P., Pedersen, M. G., et al. 2019, ApJ, 876, 4, doi: 10.3847/1538-4357/ab12df

Eiroa, C., Rebollido, I., Montesinos, B., et al. 2016, A&A, 594, L1, doi: 10.1051/0004-6361/201629514

Ekström, S., Meynet, G., Maeder, A., & Barblan, F. 2008, A&A, 478, 467, doi: 10.1051/0004-6361:20078095

Feast, M. W., Stoy, R. H., Thackeray, A. D., & Wesselink, A. J. 1961, MNRAS, 122, 239, doi: 10.1093/mnras/122.3.239

Frémat, Y., Neiner, C., Hubert, A. M., et al. 2006, A&A, 451, 1053, doi: 10.1051/0004-6361:20053305
Frémat, Y., Zorec, J., Hubert, A. M., & Floquet, M. 2005, A&A, 440, 305, doi: 10.1051/0004-6361:20042229
Garg, A., Cook, K. H., Nikolaev, S., et al. 2010, AJ, 140, 328, doi: 10.1088/0004-6256/140/2/328
Garrison, R. F., & Gray, R. O. 1994, AJ, 107, 1556, doi: 10.1086/116967
Garrison, R. F., Hiltner, W. A., & Schild, R. E. 1977, ApJS, 35, 111, doi: 10.1086/190468
Ghoreyshi, M. R., Carciofi, A. C., Rímulo, L. R., et al. 2018, MNRAS, 479, 2214, doi: 10.1093/mnras/sty1577
Gies, D. R., Bagnuolo, William G., J., Ferrara, E. C., et al. 1998, ApJ, 493, 440, doi: 10.1086/305113
Ginsburg, A., Sipőcz, B. M., Brasseur, C. E., et al. 2019, AJ, 157, 98, doi: 10.3847/1538-3881/aafc33
Granada, A., Ekström, S., Georgy, C., et al. 2013, A&A, 553, A25, doi: 10.1051/0004-6361/201220559
Green, E. M., Fontaine, G., Reed, M. D., et al. 2003, ApJL, 583, L31, doi: 10.1086/367929
Grunhut, J. H., Wade, G. A., Neiner, C., et al. 2017, MNRAS, 465, 2432, doi: 10.1093/mnras/stw2743
Handler, G. 2013, Asteroseismology, ed. T. D. Oswalt & M. A. Barstow, Vol. 4, 207, doi: 10.1007/978-94-007-5615-1_4
Hartman, J. 2012, VARTOOLS: Light Curve Analysis Program, Astrophysics Source Code Library. http://ascl.net/1208.016
Haubois, X., Carciofi, A. C., Rivinius, T., Okazaki, A. T., & Bjorkman, J. E. 2012, ApJ, 756, 156, doi: 10.1088/0004-637X/756/2/156
Hendry, E. M. 1982, PASP, 94, 169, doi: 10.1086/130958
Henize, K. G. 1976, ApJS, 30, 491, doi: 10.1086/190369
Henry, G. W., & Smith, M. A. 2012, ApJ, 760, 10, doi: 10.1088/0004-637X/760/1/10
Herbst, W., & Shevchenko, V. S. 1999, AJ, 118, 1043, doi: 10.1086/300966
Horst, L., Edelmann, P. V. F., Andrassy, R., et al. 2020, arXiv e-prints, arXiv:2006.03011. https://arxiv.org/abs/2006.03011
Huat, A. L., Hubert, A. M., Baudin, F., et al. 2009, A&A, 506, 95, doi: 10.1051/0004-6361/200911928
Iijima, T. 1985, A&A, 153, 35
Jaschek, M., & Egret, D. 1982, in IAU Symposium, Vol. 98, Be Stars, ed. M. Jaschek & H. G. Groth, 261
Kawaler, S. D., Reed, M. D., Østensen, R. H., et al. 2010, MNRAS, 409, 1509, doi: 10.1111/j.1365-2966.2010.17475.x
Kee, N. D., Owocki, S., & Sundqvist, J. O. 2016, MNRAS, 458, 2323, doi: 10.1093/mnras/stw471
Keller, S. C., Bessell, M. S., Cook, K. H., Geha, M., & Syphers, D. 2002, AJ, 124, 2039, doi: 10.1086/342548
Khalak, V. R., Romanyuk, Y. O., & Chalenko, V. E. 1998, Kinematika i Fizika Nebesnykh Tel, 14, 429
Kilkenny, D., Koen, C., O'Donoghue, D., & Stobie, R. S. 1997, MNRAS, 285, 640, doi: 10.1093/mnras/285.3.640
Klement, R., Carciofi, A. C., Rivinius, T., et al. 2019, ApJ, 885, 147, doi: 10.3847/1538-4357/ab48e7
Koch, D. G., Borucki, W. J., Basri, G., et al. 2010, ApJL, 713, L79, doi: 10.1088/2041-8205/713/2/L79
Koubský, P., Kotková, L., Votruba, V., Šlechta, M., & Dvořáková, Š. 2012, A&A, 545, A121, doi: 10.1051/0004-6361/201219679
Kouwenhoven, M. B. N., Brown, A. G. A., Portegies Zwart, S. F., & Kaper, L. 2007, A&A, 474, 77, doi: 10.1051/0004-6361:20077719
Kurtz, D. W. 1982, MNRAS, 200, 807, doi: 10.1093/mnras/200.3.807
Kurtz, D. W., Shibahashi, H., Murphy, S. J., Bedding, T. R., & Bowman, D. M. 2015, MNRAS, 450, 3015, doi: 10.1093/mnras/stv868
Labadie-Bartz, J., & Carciofi, A. C. 2020, in Proceedings of the conference Stars and their Variability Observed from Space, ed. C. Neiner, W. W. Weiss, D. Baade, R. E. Griffin, C. C. Lovekin, & A. F. J. Moffat, 185–187
Labadie-Bartz, J., Pepper, J., McSwain, M. V., et al. 2017, AJ, 153, 252, doi: 10.3847/1538-3881/aa6396
Labadie-Bartz, J., Chojnowski, S. D., Whelan, D. G., et al. 2018, AJ, 155, 53, doi: 10.3847/1538-3881/aa9c7e
Landstreet, J. D., & Borra, E. F. 1978, ApJL, 224, L5, doi: 10.1086/182746
Lee, U., Osaki, Y., & Saio, H. 1991, MNRAS, 250, 432, doi: 10.1093/mnras/250.2.432
Lee, U., & Saio, H. 2020, arXiv e-prints, arXiv:2005.00440. https://arxiv.org/abs/2005.00440
Lenz, P., & Breger, M. 2005, Communications in Asteroseismology, 146, 53, doi: 10.1553/cia146s53
Li, J. Z., Wu, C. H., Chen, W. P., et al. 2002, AJ, 123, 2590, doi: 10.1086/339971
Lightkurve Collaboration, Cardoso, J. V. d. M., Hedges, C., et al. 2018, Lightkurve: Kepler and TESS time series analysis in Python, Astrophysics Source Code Library. http://ascl.net/1812.013
Maeder, A., Grebel, E. K., & Mermilliod, J.-C. 1999, A&A, 346, 459. https://arxiv.org/abs/astro-ph/9904008
Maintz, M., Rivinius, T., Štefl, S., et al. 2003, A&A, 411, 181, doi: 10.1051/0004-6361:20031375
Meisel, D. D. 1968, AJ, 73, 350, doi: 10.1086/110637
Miroshnichenko, A. S., Bjorkman, K. S., & Krugov, V. D. 2002, PASP, 114, 1226, doi: 10.1086/342766
Moffat, A. F. J. 2008, in Clumping in Hot-Star Winds, ed. W.-R. Hamann, A. Feldmeier, & L. M. Oskinova, 17
Mourard, D., Monnier, J. D., Meilland, A., et al. 2015, A&A, 577, A51, doi: 10.1051/0004-6361/201425141

Mürset, U., & Schmid, H. M. 1999, A&AS, 137, 473, doi: 10.1051/aas:1999105
Nazé, Y., Pigulski, A., Rauw, G., & Smith, M. A. 2020, MNRAS, 494, 958, doi: 10.1093/mnras/staa617
Nazé, Y., Rauw, G., Sana, H., & Corcoran, M. F. 2013, A&A, 555, A83, doi: 10.1051/0004-6361/201321099
Neiner, C., de Batz, B., Cochard, F., et al. 2011, AJ, 142, 149, doi: 10.1088/0004-6256/142/5/149
Neiner, C., Lee, U., Mathis, S., et al. 2020, arXiv e-prints, arXiv:2007.08977. https://arxiv.org/abs/2007.08977
Neiner, C., Mathis, S., Saio, H., et al. 2012a, A&A, 539, A90, doi: 10.1051/0004-6361/201118151
Neiner, C., Floquet, M., Samadi, R., et al. 2012b, A&A, 546, A47, doi: 10.1051/0004-6361/201219820
Oudmaijer, R. D., & Parr, A. M. 2010, MNRAS, 405, 2439, doi: 10.1111/j.1365-2966.2010.16609.x
Pamyatnykh, A. A. 1999, AcA, 49, 119
Panoglou, D., Borges Fernandes, M., Baade, D., et al. 2019, MNRAS, 486, 5139, doi: 10.1093/mnras/stz1128
Panoglou, D., Carciofi, A. C., Vieira, R. G., et al. 2016, MNRAS, 461, 2616, doi: 10.1093/mnras/stw1508
Panoglou, D., Faes, D. M., Carciofi, A. C., et al. 2018, MNRAS, 473, 3039, doi: 10.1093/mnras/stx2497
Pepper, J., Kuhn, R. B., Siverd, R., James, D., & Stassun, K. 2012, PASP, 124, 230, doi: 10.1086/665044
Pepper, J., Pogge, R. W., DePoy, D. L., et al. 2007, PASP, 119, 923, doi: 10.1086/521836
Pereira, T. M. D., & Lopes, I. P. 2004, A&A, 426, 213, doi: 10.1051/0004-6361:20041181
Peters, G. J., Gies, D. R., Grundstrom, E. D., & McSwain, M. V. 2008, ApJ, 686, 1280, doi: 10.1086/591145
Peters, G. J., Wang, L., Gies, D. R., & Grundstrom, E. D. 2016, ApJ, 828, 47, doi: 10.3847/0004-637X/828/1/47
Peters, M., Wisniewski, J. P., Williams, B. F., et al. 2020, AJ, 159, 119, doi: 10.3847/1538-3881/ab6d74
Pigulski, A., & Pojmański, G. 2008, A&A, 477, 917, doi: 10.1051/0004-6361:20078581
Plavec, M. J., & Dobias, J. J. 1987, AJ, 93, 440, doi: 10.1086/114329
Poeckert, R. 1981, PASP, 93, 297, doi: 10.1086/130828
Pols, O. R., Cote, J., Waters, L. B. F. M., & Heise, J. 1991, A&A, 241, 419
Press, W. H., Teukolsky, S. A., Vetterling, W. T., & Flannery, B. P. 1992, Numerical recipes in C. The art of scientific computing
Puss, A., & Leedjärv, L. 2002, A&A, 383, 905, doi: 10.1051/0004-6361:20011809
Rainer, M., Poretti, E., Mistò, A., et al. 2016, AJ, 152, 207, doi: 10.3847/0004-6256/152/6/207
Rappaport, S., & van den Heuvel, E. P. J. 1982, in IAU Symposium, Vol. 98, Be Stars, ed. M. Jaschek & H. G. Groth, 327–344
Renson, P., & Manfroid, J. 2009, A&A, 498, 961, doi: 10.1051/0004-6361/200810788
Ricker, G. R., Winn, J. N., Vanderspek, R., et al. 2015, Journal of Astronomical Telescopes, Instruments, and Systems, 1, 014003, doi: 10.1117/1.JATIS.1.1.014003
Rieutord, M. 2009, Approaching the Low-Frequency Spectrum of Rotating Stars, Vol. 765, 101–121, doi: 10.1007/978-3-540-87831-5_4
Rímulo, L. R., Carciofi, A. C., Vieira, R. G., et al. 2018, MNRAS, 476, 3555, doi: 10.1093/mnras/sty431
Rivinius, T., Baade, D., & Carciofi, A. C. 2016, A&A, 593, A106, doi: 10.1051/0004-6361/201628411
Rivinius, T., Baade, D., Hadrava, P., Heida, M., & Klement, R. 2020, A&A, 637, L3, doi: 10.1051/0004-6361/202038020
Rivinius, T., Baade, D., Stefl, S., et al. 1998a, A&A, 333, 125
Rivinius, T., Baade, D., Stefl, S., et al. 1998b, in Astronomical Society of the Pacific Conference Series, Vol. 135, A Half Century of Stellar Pulsation Interpretation, ed. P. A. Bradley & J. A. Guzik, 343
Rivinius, T., Baade, D., & Štefl, S. 2003, A&A, 411, 229, doi: 10.1051/0004-6361:20031285
Rivinius, T., Carciofi, A. C., & Martayan, C. 2013, A&A Rv, 21, 69, doi: 10.1007/s00159-013-0069-0
Roberts, M. S. 1962, AJ, 67, 79, doi: 10.1086/108603
Rogers, T. M., Lin, D. N. C., McElwaine, J. N., & Lau, H. H. B. 2013, ApJ, 772, 21, doi: 10.1088/0004-637X/772/1/21
Romanyuk, I. I., & Kudryavtsev, D. O. 2008, Astrophysical Bulletin, 63, 139, doi: 10.1134/S1990341308020053
Rosales Guzmán, J. A., Mennickent, R. E., Djurašević, G., Araya, I., & Curé, M. 2018, MNRAS, 476, 3039, doi: 10.1093/mnras/sty224
Sahoo, S. K., Baran, A. S., Heber, U., et al. 2020, MNRAS, 495, 2844, doi: 10.1093/mnras/staa1337
Saio, H. 2013, Prospects for Asteroseismology of Rapidly Rotating B-Type Stars, ed. M. Goupil, K. Belkacem, C. Neiner, F. Lignières, & J. J. Green, Vol. 865, 159, doi: 10.1007/978-3-642-33380-4_8
Saio, H., Bedding, T. R., Kurtz, D. W., et al. 2018a, MNRAS, 477, 2183, doi: 10.1093/mnras/sty784
Saio, H., Kurtz, D. W., Murphy, S. J., Antoci, V. L., & Lee, U. 2018b, MNRAS, 474, 2774, doi: 10.1093/mnras/stx2962
Saio, H., Cameron, C., Kuschnig, R., et al. 2007, ApJ, 654, 544, doi: 10.1086/509315
Samus', N. N., Kazarovets, E. V., Durlevich, O. V., Kireeva, N. N., & Pastukhova, E. N. 2017, Astronomy Reports, 61, 80, doi: 10.1134/S1063772917010085

Secchi, A. 1866, Astronomische Nachrichten, 68, 63, doi: 10.1002/asna.18670680405
Semaan, T., Hubert, A. M., Zorec, J., et al. 2018, A&A, 613, A70, doi: 10.1051/0004-6361/201629243
Shokry, A., Rivinius, T., Mehner, A., et al. 2018, A&A, 609, A108, doi: 10.1051/0004-6361/201731536
Shultz, M. E., Wade, G. A., Rivinius, T., et al. 2019, MNRAS, 485, 1508, doi: 10.1093/mnras/stz416
Sigut, T. A. A., & Patel, P. 2013, ApJ, 765, 41, doi: 10.1088/0004-637X/765/1/41
Simón-Díaz, S., Aerts, C., Urbaneja, M. A., et al. 2018, A&A, 612, A40, doi: 10.1051/0004-6361/201732160
Skiff, B. A. 2009, VizieR Online Data Catalog
—. 2013, VizieR Online Data Catalog
Slettebak, A. 1982, ApJS, 50, 55, doi: 10.1086/190820
Smith, M. A., Henry, G. W., & Vishniac, E. 2006, ApJ, 647, 1375, doi: 10.1086/505564
Sota, A., Maíz Apellániz, J., Morrell, N. I., et al. 2014, ApJS, 211, 10, doi: 10.1088/0067-0049/211/1/10
Stankov, A., & Handler, G. 2005, ApJS, 158, 193, doi: 10.1086/429408
Stephenson, C. B., & Sanduleak, N. 1971, Publications of the Warner & Swasey Observatory, 1, 1
Sterken, C., Vogt, N., & Mennickent, R. 1994, A&A, 291, 473
Sterken, C., Vogt, N., & Mennickent, R. E. 1996a, A&A, 311, 579
—. 1996b, Information Bulletin on Variable Stars, 4311, 1
Thackeray, A. D., Alexander, J. B., & Hill, P. W. 1970, Information Bulletin on Variable Stars, 483, 1
Thaller, M. L., Bagnuolo, William G., J., Gies, D. R., & Penny, L. R. 1995, ApJ, 448, 878, doi: 10.1086/176016
The, P. S., de Winter, D., & Perez, M. R. 1994, A&AS, 104, 315
Touhami, Y., Gies, D. R., & Schaefer, G. H. 2011, ApJ, 729, 17, doi: 10.1088/0004-637X/729/1/17
Štefl, S., Baade, D., Rivinius, T., et al. 1998, in Astronomical Society of the Pacific Conference Series, Vol. 135, A Half Century of Stellar Pulsation Interpretation, ed. P. A. Bradley & J. A. Guzik, 348
VanderPlas, J., Connolly, A. J., Ivezic, Z., & Gray, A. 2012, in Proceedings of Conference on Intelligent Data Understanding (CIDU, 47–54, doi: 10.1109/CIDU.2012.6382200
VanderPlas, J. T., & Ivezić, Ž. 2015, ApJ, 812, 18, doi: 10.1088/0004-637X/812/1/18
Vanzi, L., Chacon, J., Helminiak, K. G., et al. 2012, MNRAS, 424, 2770, doi: 10.1111/j.1365-2966.2012.21382.x
Varga, J., Gerják, T., Ábrahám, P., et al. 2019, MNRAS, 485, 3112, doi: 10.1093/mnras/stz486
Vennes, S., Kawka, A., Jonić, S., et al. 2011, MNRAS, 413, 2760, doi: 10.1111/j.1365-2966.2011.18350.x
Vieira, R. G., Carciofi, A. C., Bjorkman, J. E., et al. 2017, MNRAS, 464, 3071, doi: 10.1093/mnras/stw2542
Voges, W., Aschenbach, B., Boller, T., et al. 1999, A&A, 349, 389. https://arxiv.org/abs/astro-ph/9909315
Wade, G. A., Petit, V., Grunhut, J. H., Neiner, C., & MiMeS Collaboration. 2016, in Astronomical Society of the Pacific Conference Series, Vol. 506, Bright Emissaries: Be Stars as Messengers of Star-Disk Physics, ed. T. A. A. Sigut & C. E. Jones, 207
Walker, G., Matthews, J., Kuschnig, R., et al. 2003, PASP, 115, 1023, doi: 10.1086/377358
Walker, G. A. H., Kuschnig, R., Matthews, J. M., et al. 2005a, ApJL, 635, L77, doi: 10.1086/499362
—. 2005b, ApJL, 623, L145, doi: 10.1086/430254
Wang, L., Gies, D. R., & Peters, G. J. 2018, ApJ, 853, 156, doi: 10.3847/1538-4357/aaa4b8
Weiss, W. W., Rucinski, S. M., Moffat, A. F. J., et al. 2014, PASP, 126, 573, doi: 10.1086/677236
Wheelwright, H. E., Oudmaijer, R. D., & Schnerr, R. S. 2009, A&A, 497, 487, doi: 10.1051/0004-6361/200811105
Wisniewski, J. P., & Bjorkman, K. S. 2006, ApJ, 652, 458, doi: 10.1086/507260
Zechmeister, M., & Kürster, M. 2009, A&A, 496, 577, doi: 10.1051/0004-6361:200811296
Zhang, P., Chen, P. S., & Yang, H. T. 2005, NewA, 10, 325, doi: 10.1016/j.newast.2004.12.002
Ziolkowski, J. 2002, Mem. Soc. Astron. Italiana, 73, 1038. https://arxiv.org/abs/astro-ph/0208455
Zorec, J., & Briot, D. 1997, A&A, 318, 443